Acta Astronautica 188 (2021) 151–170

Contents lists available at ScienceDirect

Acta Astronautica

journal homepage: www.elsevier.com/locate/actaastro

Research paper

Multi-criteria design of continuous global coverage Walker and Street-of-Coverage constellations through property assessment

S. Huang [*,1], C. Colombo [2], F. Bernelli-Zazzera [3]

Politecnico di Milano, Milan, 20156, Italy

ARTICLE INFO

Keywords:
Continuous global coverage constellation
Walker constellation
Street-of-Coverage constellation
Multi-criteria constellation design

ABSTRACT

No general rules exist for constellation design; instead, constellation designers have to consider various cost drivers in a trade-off way. This paper presents a systematic method for the design of continuous global coverage Walker and Street-of-Coverage constellations, by taking seven critical constellation properties (coverage, robustness, self-induced collision avoidance, launch, build-up, station-keeping, and end-of-life disposal) as design criteria. In this method, a set of characteristic parameters, which can determine the constellation configuration, are first identified based on the review of Walker and Street-of-Coverage constellations. Then a series of indexes are proposed and modelled as functions of the characteristic parameters, to quantitatively assess the constellation properties. Through the quantitative assessment, the influence of constellation configuration on constellation properties are revealed, and the trade-offs between constellation properties are analysed. Finally, taking the characteristic parameters and constellation properties as the design variables and objectives, a multi-objective optimisation problem is formulated to find the globally optimal constellations for given missions.

1. Introduction

As services from space are becoming an asset for life on the Earth and the demand for data from space increases, the international interest in satellite constellations is increasingly growing. A satellite constellation is "*a set of satellites distributed over space intended to work together to achieve common objectives*" [1, page 671]. It is well known that the characteristics of different constellations vary dramatically, and constellations can fall into various categories depending on the type of coverage (continuous/intermittent), the type of coverage region (global/zonal), the type of orbit (circular/elliptical/hybrid), the altitude of implementation (low/medium/geosynchronous Earth orbit), etc. In this paper, we will perform a general study of global coverage constellations, which are often used for telecommunications, navigation and positioning, and other similar functions [1, page 671], and particularly, we are focused on circular-orbit and continuous coverage constellations in which all satellites are placed at common altitude and inclination.

An Earth-orbiting constellation can be applied to surveillance and reconnaissance, telecommunications, positioning and navigation, military defence, etc. For continuous global coverage constellations, depending on the service to be offered, the required coverage fold can be from one to four, where the coverage fold refers to the minimum number of satellites continuously visible to every point on the Earth's surface. In general, most of the missions in Low Earth Orbit (LEO) require 1-fold coverage to offer surveillance and reconnaissance, and telecommunications services, whereas the missions in Medium Earth Orbit (MEO) usually require 4-fold coverage to offer positioning and navigation services. Moreover, thanks to the development of material technologies, some novel constellations have been proposed. For example, Pan et al. [2,3] designed a navigation constellation around the Sun–Earth+Moon Artificial Lagrange Points, in which satellites were replaced by solar sails; the major design criterion was to reduce the lightness number of solar sail's motion.

Over the past decades, different types of circular-orbit constellations have been proposed, such as Walker, Street-of-Coverage, and Flower. The Walker constellation was first published by Walker [4–7] in 1970s. It is also reported in Ref. [8] that Mozhaev [9,10] had independently proposed the similar constellation in 1968. The Walker constellation is characterised by a globally symmetrical structure, in which all satellites and orbital planes are uniformly distributed. Then researchers such as Ballard, Lang, and Adams [11–14] conducted fruitful work, finding the optimal Walker constellations providing continuous global coverage

* Corresponding author.
E-mail addresses: simeng.huang@polimi.it (S. Huang), camilla.colombo@polimi.it (C. Colombo), franco.bernelli@polimi.it (F. Bernelli-Zazzera).
[1] Ph.D. Candidate, Department of Aerospace Science and Technology.
[2] Associate Professor, Department of Aerospace Science and Technology.
[3] Full Professor, Department of Aerospace Science and Technology

https://doi.org/10.1016/j.actaastro.2021.07.002
Received 4 August 2020; Received in revised form 22 May 2021; Accepted 2 July 2021
Available online 15 July 2021
0094-5765/© 2021 The Authors. Published by Elsevier Ltd on behalf of IAA. This is an open access article under the CC BY-NC-ND license (http://creativecommons.org/licenses/by-nc-nd/4.0/).

Nomenclature

Acronyms

AoL	Argument of Latitude
ECI	Earth Centred Inertial
EoL	End-of-Life
GPS	Global Positioning System
LEO	Low Earth Orbit
MEO	Medium Earth Orbit
PU	Pattern Unit
RAAN	Right Ascension of the Ascending Node
SoC	Street-of-Coverage

Constants

Earth mean equatorial radius $R_\oplus \approx 6378.16$ km
Earth gravitational parameter $\mu \approx 3.9860 \times 10^5$ km^3/s^2

Symbols

a_f	semi-major axis after altitude decay, km
a_g	semi-major axis of the graveyard orbit, km
a_n	semi-major axis of the nominal orbit, km
a^*	reference semi-major axis, km
bld	index to assess the build-up property
C_j^θ	half-width of SoC required for j-fold continuous coverage, rad or deg
C_j^ϑ	minimum half-width of SoC required for j-fold continuous global coverage, rad or deg
cov	excess coverage
F	phasing parameter
h	altitude, km
h_{pd}	perigee altitude of the disposal orbit, km
h_s	scale height, km
i	inclination, rad or deg
j	coverage fold
J_1	objective function of the coverage property
J_2	objective function of the robustness property
J_3	objective function of the self-induced collision avoidance property
J_4	objective function of the launch property
J_5	objective function of the build-up property
J_6	objective function of the station-keeping property
$(J_7)_{\text{LEO}}$	objective function of the EoL disposal property for the LEO mission
$(J_7)_{\text{MEO}}$	objective function of the EoL disposal property for the MEO mission
$\boldsymbol{J}_{\text{LEO}}$	objective vector for the LEO mission
$\boldsymbol{J}_{\text{MEO}}$	objective vector for the MEO mission
lch_h	index to assess the launch property, km
lch_i	index to assess the launch property, rad or deg
$m/C_D A$	ballistic coefficient, kg/m^2
N	number of satellites
opp	unit collision opportunity, s^{-1}
P	number of orbital planes
pct	average percentage of the Earth's surface visible to $(j+1)$ satellites over one orbit period, %
r_{pd}	perigee radius of the disposal orbit, km
S	number of satellites per orbital planes
T	unperturbed orbit period, s
$\boldsymbol{x}_{\text{Walker}}$	design variable vector for the Walker constellation
$\boldsymbol{x}_{\text{SoC}}$	design variable vector for the SoC constellation
θ	angular radius of the footprint, rad or deg
ϑ	central angle of coverage, rad or deg
ρ	atmospheric density, kg/km^3
ρ^*	reference atmospheric density, kg/km^3
Δu_{inter}	inter-plane AoL spacing between successive satellites in adjacent orbital planes, rad or deg
Δu_{intra}	intra-plane AoL spacing between satellites in a single orbital plane, rad or deg
$\Delta u_{\text{s/c}}$	AoL spacing between satellites, rad or deg
Δv_{keep}	Δv-budget of a constellation for station-keeping, km/s
$(\Delta v_{\text{EoL}})_{\text{LEO}}$	Δv-budget of a LEO constellation for EoL disposal, km/s
$(\Delta v_{\text{EoL}})_{\text{MEO}}$	Δv-budget of a MEO constellation for EoL disposal, km/s
$\Delta\Omega$	RAAN spacing between adjacent orbital planes, rad or deg
$\Delta\Omega_{\text{co}}$	RAAN spacing between adjacent orbital planes with co-rotating interface for the SoC constellation, rad or deg
$\Delta\Omega_{\text{counter}}$	RAAN spacing between adjacent orbital planes with counter-rotating interface for the SoC constellation, rad or deg
$\Delta\Omega_{\text{s/c}}$	RAAN spacing between satellites, rad or deg
ϵ	elevation angle, rad or deg
ϕ_{site}	latitude of the launch site, rad or deg
ψ	satellite-pair miss distance, rad or deg
Ψ	constellation miss distance

Subscripts

lb	lower bound
min	minimum value
ub	upper bound

with a minimum number of satellites. The Street-of-Coverage (SoC) constellation was developed based on a Street-of-Coverage (SoC) concept, where the SoC refers to a swath on the ground with continuous coverage. At the early stage of SoC constellation design, the orbits were evenly spaced along the equatorial plane, and some work [15–17] was devoted to finding the optimal number of orbits and inclinations required to cover the zone of interest [14]. In 1978, Beste [18] proposed the polar SoC constellation in which polar orbits were unevenly spaced; compared to an early work by Lüders [15], Beste reduced the number of satellites by 15% for 1-fold continuous global coverage [18]. Then Rider [19] carried out a further study to find the optimal polar SoC constellations providing continuous global coverage with a minimum number of satellites. However, the polar SoC constellation does not suit practical applications because all orbits cross at the poles, thus may leading to high collision hazards. In order to address this problem, Ulybyshev [8] proposed the near-polar SoC constellation by transforming the original polar constellations to a new class of inclined ones. The Flower constellation was proposed by Mortari et al. [20] in 2004. It is a theoretical framework that allows the design of symmetrical constellations whose satellites all move on the same trajectory with respect to a rotating reference frame. Based on the original Flower constellation, the 2D and 3D Lattice Flower constellations were developed [21,22], encompassing the Walker constellation and some other symmetrical constellations with elliptical orbits.

Traditionally, the prime design criterion for continuous global coverage constellations is the coverage performance. A good coverage performance can guarantee the quality of communications between ground and constellation, and it usually indicates fewer satellites required, thus reducing the system cost. However, the mono-criterion design may not suit practical applications, because the design of constellations is a complicated trade-off process during which various cost drivers have to be taken into account. Draim and Kacena [23] discussed the impacts on constellation design from various aspects: launch vehicle, orbit maintenance, debris, etc. Lang and Adams [14] compared the Walker, polar SoC, and Draim constellations in terms of coverage, launch vehicle capability, spare strategy, crosslinking, and space debris mitigation and collision avoidance. Lansard and Palmade [24] proposed a multi-criteria approach, highlighting and handling three driving criteria: coverage performance, operational availability, and life-cycle costs of the system. Lansard et al. [25] incorporated the robustness consideration and some additional coverage constraints, and designed a new type of constellation which was resistant to satellite failures by using an optimisation tool based on genetic algorithms. Keller et al. [26] examined the polar and near-polar constellations for the use of intersatellite links. Ferringer and Spencer [27] studied two pairs of trade-offs – sparse-coverage trade-off and resolution trade-off – using multi-objective evolutionary computation. Li et al. [28] proposed a general evaluation criterion for the coverage of LEO constellations, which was applicable to different constellation configurations. Shtark and Gurfil [29] developed a LEO constellation optimisation method for regional positioning, and examined the figures of merit of total coverage time, revisit time, and geometric dilution of precision percentiles. Buzzi et al. [30] described the process of constellation and orbit design for the TROPICS mission, in which the following figures of merit were assessed: coverage, cost, constellation robustness, lifetime, and deployment. It has to be noted that the aforementioned work is not limited to the study scope of this paper, viz. circular-orbit continuous global coverage constellations, but they are reviewed for the purpose of identifying the critical criteria for constellation design along with the approaches of modelling the criteria.

In this paper, a multi-criteria design of circular-orbit continuous global coverage constellations is presented, with the major objective to develop a systematic constellation design method to maximise constellation performances and to minimise costs. The development of this method is generally divided into three steps.

First, we choose two classical types of circular-orbit constellations: Walker and SoC, and perform a thorough review of their characteristics; this choice is justified by the fact that many practical applications (e.g. the Galileo [31] and Iridium [32,33] constellations) are of these types. Based on the review, a set of characteristic parameters, which can determine the configuration of a Walker or SoC constellation, are identified. Note that a contribution of this paper to the literature is deriving the necessary condition for continuous global coverage for the SoC constellation.

Then by widely reviewing the previous work on constellation design, we select seven constellation properties as design criteria, each of them representing a particular constellation performance or cost, reported in Table 1. Because these performances and costs are constellation's inherent qualities, they are collectively called here as constellation properties. For each property, one or two indexes are proposed with valid reasons, and the indexes are modelled as functions of the characteristic parameters that having been identified. In this way, we can quantitatively establish the relationship between constellation configuration and properties through mathematical formulas, and furthermore, analyse the trade-offs between properties; recall that the constellation configuration is represented by the characteristic parameters.

Finally, taking the constellation properties as objectives and taking the characteristic parameters as design variables, a multi-objective optimisation problem is formulated, in which the mission-related parameters can be replaced according to given mission requirements. With the help of multi-objective optimisation techniques, the globally optimal constellations for a given mission can be found.

Note that the study scope of this paper, apart from the circular-orbit continuous global coverage constellations in Walker and SoC types, is focused on analysing the prograde-orbit constellations containing no more than 200 satellites. Besides, due to space limitations, in the paper we only present the results for 1- and 4-fold coverage LEO and MEO constellations; however, the systematic constellation design method developed can also be applied to 2- or 3-fold coverage and to geosynchronous constellations.

The remainder of this paper is organised as follows. Section 2 presents a thorough review of Walker and SoC constellations, based on which, the characteristic parameters are identified, reported in Section 3. Section 4 quantitatively assesses the constellation properties using the characteristic parameters, and analyses the trade-offs between properties. Finally, a multi-objective optimisation problem is formulated in Section 5 to find the globally optimal constellations for given missions.

2. Review of Walker and Street-of-Coverage constellations for continuous global coverage

The Walker and SoC constellations are two typical types of constellations that have been widely studied. The common characteristics of these two types of constellations are:

(1) the constellation, containing a total of N satellites, is composed of S satellites evenly spaced on each of P orbital planes;
(2) all satellites are placed in circular orbits at the same altitude h and at the same inclination i.

On the other hand, the essential difference between these two types of constellations is the distribution of orbital planes, which will be shown in the following sections.

Note that, although in Section 3 we will present the characteristic parameters which can determine the configuration of a Walker or SoC constellation, we list them here for ease of understanding, viz. N, P, h, i, and a phasing parameter (for the Walker constellation only). If not specified, all other parameters appearing in the following sections are dependent on the characteristic parameters.

2.1. Walker constellations

The Walker constellation is globally symmetrical in terms of the geometrical configuration. When describing a Walker constellation, a Pattern Unit (PU) is used to measure angular distances within the constellation, with 1 PU = $2\pi/N$ rad [6].

The characteristics of a Walker constellation are defined as follows [6].

(1) All the P orbital planes are evenly spaced along the equatorial plane at intervals of S PUs.
(2) In each orbital plane, the S satellites are evenly spaced at intervals of P PUs.

Table 1
Constellation properties.

Property	Description
Coverage	Performance to offer required coverage
Robustness	Performance to offer required coverage if satellite fails
Self-induced collision avoidance	Performance to avoid collision between satellites from the same constellation
Launch	Cost to deliver constellation to mission orbit
Build-up	Period to build up constellation
Station-keeping	Cost to maintain constellation structure
End-of-Life (EoL) disposal	Cost to remove constellation from mission orbit

(3) When a satellite is at its ascending node, some satellite in the adjacent orbital plane towards east has an Argument of Latitude (AoL) of F PUs, where F is an integer which may have any value from 0 to $(P-1)$.[4]

To summarise, the distribution of orbital planes and satellites for a Walker constellation can be described by

$$\Delta\Omega = S, \quad \Delta u_{\text{intra}} = P, \quad \Delta u_{\text{inter}} = F \tag{1}$$

where $\Delta\Omega$ is the Right Ascension of the Ascending Node (RAAN) spacing between adjacent orbital planes, Δu_{intra} is the intra-plane AoL spacing between adjacent satellites in a single orbital plane, and Δu_{inter} is the inter-plane AoL spacing between successive satellites in adjacent orbital planes, with the term "successive" referring to satellites *successively* passing their respective ascending nodes.

A Walker constellation can be designated in shorthand notation as i: $N/P/F$ [6]. Two typical Walker constellations are the 55 deg: 24/6/2 Global Positioning System (GPS) constellation [34] and the 56 deg: 24/3/1 Galileo constellation [31].

2.2. Street-of-Coverage constellations

The SoC constellation is a class of asymmetrical constellations in terms of the geometrical configuration, in which orbital planes are unevenly spaced either along the equatorial plane or along half of the equatorial plane [8,18,19]. It has been demonstrated by Ulybyshev [8] that the former configuration generally consists of more orbital planes with fewer satellites per orbital plane than the latter one. In this study we focus on the latter configuration, i.e., orbital planes unevenly spaced along half of the equatorial plane, for the reason that we will take into account the build-up property for the present constellation design, and this property degrades with the number of orbital planes (see Section 4.5).

2.2.1. Geometrical configuration

There exist two types of interfaces between orbital planes in the SoC constellation: the co-rotating interface and the counter-rotating interface. The co-rotating interface is such that satellites in adjacent orbital planes move in the same direction. The counter-rotating interface is such that satellites in adjacent orbital planes move in the opposite directions [8]. Fig. 1 shows an illustrative example of a polar SoC constellation (i.e. $i = 90$ deg) consisting of four orbital planes, where the arrows indicate the direction of satellite motion and $\Delta\Omega_{\text{co}}$, $\Delta\Omega_{\text{counter}}$ are the RAAN spacings between adjacent orbital planes with co- and counter-rotating interfaces, respectively. As shown in the figure, the co-rotating interfaces exist between plane 1 and 2, plane 2 and 3, and plane 3 and 4, whereas the counter-rotating interface exists between plane 4 and 1. Having the concept of co- and counter-rotating interfaces, the superiority of the SoC constellation can be described as follows: the coverage overlap on the co-rotating interface is minimised at the maximum perpendicular distance between adjacent orbital planes, where the maximum perpendicular distance occurs at 90 deg on either side of the intersection of two orbits [1, Sec. 13.1]. A detailed explanation of the coverage geometry of the co- and counter-rotating interfaces is presented in Appendix B.

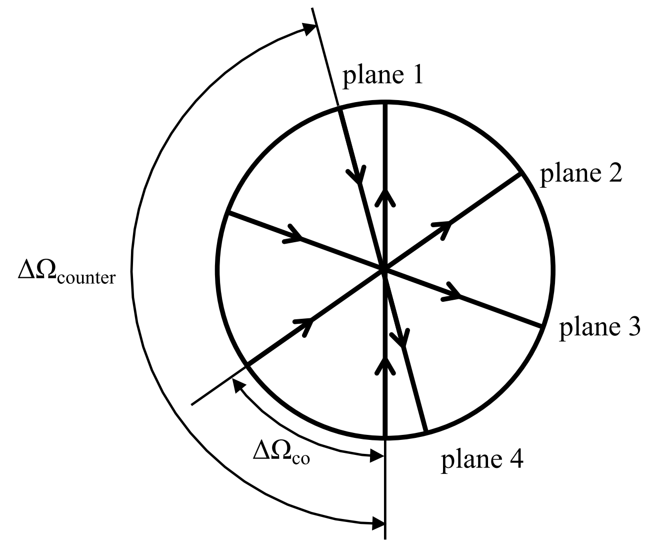

Fig. 1. Illustration of the co- and counter-rotating interfaces from polar view, assuming a polar SoC constellation consisting of four orbital planes.

The characteristics of a SoC constellation are defined as follows.

(1) The RAAN spacings between adjacent orbital planes with co- and counter-rotating interfaces, denoted by $\Delta\Omega_{\text{co}}$ and $\Delta\Omega_{\text{counter}}$, are given by [8] [1, Sec. 13.1]

$$\Delta\Omega_{\text{co}} = 2\sin^{-1}\left(\sin\frac{\vartheta + C_j^{\vartheta}}{2} \Big/ \sin i\right), \quad \Delta\Omega_{\text{counter}} = 2\sin^{-1}\left(\sin\frac{\pi - C_1^{\vartheta} - C_j^{\vartheta}}{2} \Big/ \sin i\right) \tag{2}$$

where ϑ is the central angle of coverage and C_j^{ϑ} is the minimum half-width of Street-of-Coverage (SoC) required for j-fold continuous global coverage, with $j = 1$ to 4 being the coverage fold. Note that j is not dependent on the characteristic parameters but specified by the mission requirement. A detailed description of the coverage geometry of the SoC concept is given in Appendix A. ϑ and C_j^{ϑ} are related by [8,18,19]

$$\cos\vartheta = \cos C_j^{\vartheta} \cos(j\pi/S) \tag{3}$$

As a matter of fact, the central angle of coverage is a shared concept for both Walker and SoC constellations; the definition and discussion of ϑ will be presented in Section 2.3. In addition, there is geometrical constraint for $\Delta\Omega_{\text{co}}$ and $\Delta\Omega_{\text{counter}}$ [8] [1, Sec. 13.1]:

$$\Delta\Omega_{\text{counter}} = (P-1)\,\Delta\Omega_{\text{co}} \le \pi \tag{4}$$

because all orbital planes have to be placed within half of the equatorial plane; if $\Delta\Omega_{\text{counter}} = \pi$, then the two orbital planes

[4] F can also be equal to or larger than P, but then the configuration of the constellation will be the same as $F = F - P$.

with counter-rotating interface will intersect at the equatorial plane [8].

(2) In each orbital plane, the S satellites are evenly spaced at intervals of $2\pi/S$ rad, i.e.:

$$\Delta u_{\text{intra}} = 2\pi/S \tag{5}$$

(3) When a satellite is at its ascending node, some satellite in the adjacent orbital plane towards east has an AoL of [8]

$$u = \Delta u_{\text{inter}} = j\pi/S - 2\cos^{-1}\left(\cos\frac{\Delta\Omega_{\text{co}}}{2} / \cos\frac{\vartheta + C_j^{\vartheta}}{2}\right) \tag{6}$$

A SoC constellation in this study is designated in shorthand notation as i: N/P. A typical SoC constellation is the 86.4 deg: 66/6 Iridium constellation [32,33].

2.2.2. Necessary condition for continuous global coverage

One significant advantage of the SoC constellation is the superiority in terms of the coverage overlap, which however, imposes a constraint on the number of orbital planes. In the following a demonstration of this concept will be given.

Supposing that a polar SoC constellation with N satellites and P orbital planes is able to offer j-fold continuous global coverage, there must be

$$S\vartheta \geq j\pi \tag{7}$$

$$(P-1)\left(\vartheta + C_j^{\vartheta}\right) \leq \pi \tag{8}$$

where the first inequality implies that the coverage is continuous along the SoC for every orbital plane (see Appendix A for detail), and the second inequality is derived by substituting Eq. (2) into Eq. (4) (assuming i = 90 deg), indicating that all orbital planes are placed within half of the equatorial plane. From Eq. (7) and (8), the following inequality holds:

$$S\vartheta \geq j(P-1)\left(\vartheta + C_j^{\vartheta}\right) \tag{9}$$

Replacing S with N/P, after some manipulations, Eq. (9) becomes

$$[N - jP(P-1)]\,\vartheta \geq jP(P-1)\,C_j^{\vartheta} \tag{10}$$

Observing from Eq. (10) that the right-hand side is non-negative, so the left-hand side must be non-negative too. And therefore, we have

$$jP(P-1) \leq N \tag{11}$$

Eq. (11) is a necessary condition for a polar SoC constellation able to offer j-fold continuous global coverage; that is to say, if a polar SoC constellation does not satisfy Eq. (11), then it cannot offer the required coverage.[5] Since a polar SoC constellation is always more efficient in terms of the coverage performance than the inclined ones with the same number of satellites and orbital planes [8], if a polar SoC constellation cannot offer the required coverage, neither can the similar inclined ones. To conclude, the SoC constellation that does not satisfy Eq. (11) should be removed during the preliminary design.

2.3. Central angle of coverage

Fig. 2 illustrates the coverage geometry of a single satellite, where $R_\oplus \approx 6378.16$ km is the Earth mean equatorial radius, θ is the angular radius of the footprint, ϑ is the minimum angular radius of the footprint required for a specified fold of continuous global coverage, called here as the central angle of coverage, and ϵ is the elevation angle measured at the edge of the footprint, representing the worst

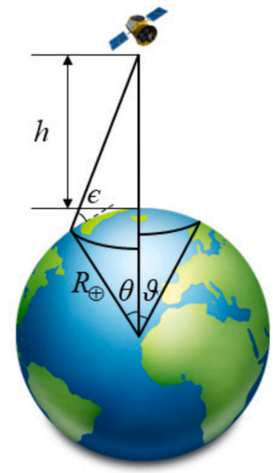

Fig. 2. Coverage geometry of a single satellite.

communication condition from the ground. Note that ϵ is not dependent on the characteristic parameters. h, θ, and ϵ are related by

$$\frac{\cos(\theta + \epsilon)}{\cos\epsilon} = \frac{R_\oplus}{h + R_\oplus} \tag{12}$$

Note that θ must be less than 90 deg otherwise h will be infinite.

Different than θ which is relevant to h, ϑ is independent of h but can be uniquely determined for a Walker constellation with given N, P, F, i, or for a SoC constellation with given N, P, and i; the approaches to determining ϑ for Walker and SoC constellations are presented in Appendix C. Once ϑ is determined, from Eq. (12), the lower bound for h required for a specified fold of continuous global coverage can be obtained, if ϵ is given:

$$h \geq h_{\text{lb}} = \left[\frac{\cos\epsilon}{\cos(\vartheta + \epsilon)} - 1\right] R_\oplus \tag{13}$$

Figs. 3 and 4 show the minimum central angles of coverage required for 1- and 4-fold continuous global coverage for given numbers of satellites and orbital planes, for Walker and SoC constellations, respectively. Here the minimum ϑ for given N and P is obtained by varying F from 0 to $(P-1)$ (Walker only) and by varying i from 0 deg to 90 deg. In other words, each point of the plots represents a particular i: $N/P/F$ Walker or i: N/P SoC constellation, whose ϑ is the smallest among the constellations with the same N and P. Especially, for the SoC constellation, given N and P, the minimum ϑ is always provided by the polar one [8].

As shown in the figures, for both Walker and SoC constellations, the minimum central angle of coverage, or the lower bound for the altitude (see Eq. (13)), generally decreases with the number of satellites and orbital planes.

3. Characteristic parameters of Walker and Street-of-Coverage constellations

Based on the review in Section 2, a set of characteristic parameters, which can determine the configuration of a Walker or SoC constellation, are identified, reported in Table 2; they are: the number of satellites N, the number of orbital planes P, the phasing parameter F (for the Walker constellation only), the inclination i, and the altitude h. With these parameters, all geometrical information, such as the distribution of orbital planes, the relative positions of satellites, and the central angle of coverage, can be obtained. Note that in this study the elevation angle is assumed constant; this assumption defines a lower bound for communication quality between ground and constellation. As indicated in the table, compared to the Walker constellation, the SoC

[5] If a proposition is true, then its converse-negative proposition must be true.

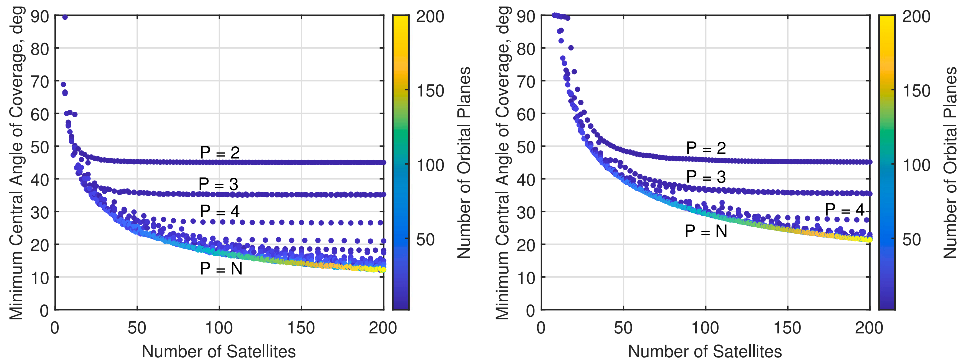

(a) **1-fold continuous global coverage.**

(b) **4-fold continuous global coverage.**

Fig. 3. Minimum central angles of coverage for given numbers of satellites and orbital planes, for the Walker constellation (the number of orbital planes increasing as the colour from dark to light).

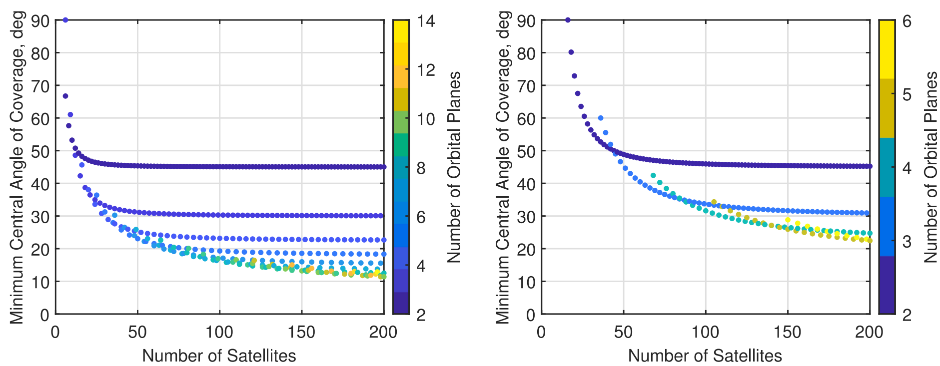

(a) **1-fold continuous global coverage.**

(b) **4-fold continuous global coverage.**

Fig. 4. Minimum central angles of coverage for given numbers of satellites and orbital planes, for the SoC constellation (the number of orbital planes increasing as the colour from dark to light).

Table 2
Characteristic parameters.

Parameter	Symbol	Constellation
Number of satellites	N	Walker, SoC
Number of orbital planes	P	Walker, SoC
Phasing parameter	F	Walker
Inclination	i	Walker, SoC
Altitude	h	Walker, SoC

constellation lacks of a design parameter F, due to the design logic to minimise the coverage overlap on the co-rotating interface at the maximum perpendicular distance between adjacent orbital planes. In the followings we will show how to obtain the depended geometrical parameters from the characteristic parameters, taking as example the GPS, Galileo, and Iridium constellations.

Table 3 gives the geometrical information of the GPS and Galileo constellations offering 4-fold continuous global coverage. In the table:

- the characteristic parameters are taken from Ref. [34] and Ref. [31];
- $\Delta\Omega$, $\Delta u_{\mathrm{intra}}$, and $\Delta u_{\mathrm{inter}}$ are derived from Eq. (1);
- ϑ is determined using the "test point" approach presented in Appendix C.1;
- θ is derived from Eq. (12), assuming $\epsilon = 5$ deg.

Figs. 5(a) and 5(b) show the configurations of the GPS and Galileo constellations, respectively, in the Earth Centred Inertial (ECI) coordinate system, where the round markers and lines indicate the satellites and orbital planes, respectively.

Table 3
Geometrical information of the GPS and Galileo constellations.

Parameter	Symbol	Value	
		GPS	Galileo
Number of satellites	N	24	24
Number of orbital planes	P	6	3
Number of satellites per orbital plane	S	4	8
Phasing parameter	F	2	1
Inclination	i	55 deg	56 deg
Altitude	h	20,200 km	23,222 km
RAAN spacing	$\Delta\Omega$	4 PU (60 deg)	8 PU (120 deg)
Intra-plane AoL spacing	$\Delta u_{\mathrm{intra}}$	6 PU (90 deg)	3 PU (45 deg)
Inter-plane AoL spacing	$\Delta u_{\mathrm{inter}}$	2 PU (30 deg)	1 PU (15 deg)
Central angle of coverage	ϑ	57.6 deg	55.7 deg
Angular radius of the footprint	θ	71.2 deg	72.6 deg

Table 4 gives the geometrical information of the Iridium constellation offering 1-fold continuous global coverage. In the table:

- the characteristic parameters are taken from Ref. [32] and Ref. [33];
- $\Delta\Omega_{\mathrm{co}}$, $\Delta\Omega_{\mathrm{counter}}$, $\Delta u_{\mathrm{intra}}$, and $\Delta u_{\mathrm{inter}}$ are derived from Eqs. (2) – (6), and they are consistent with the data in Ref. [32] and Ref. [33];
- ϑ is determined using the approach presented in Appendix C.2;
- θ is derived from Eq. (12), assuming $\epsilon = 5$ deg.

Fig. 6 shows the configuration of the Iridium constellation in the ECI coordinate system, where the round markers and lines indicate the satellites and orbital planes, respectively.

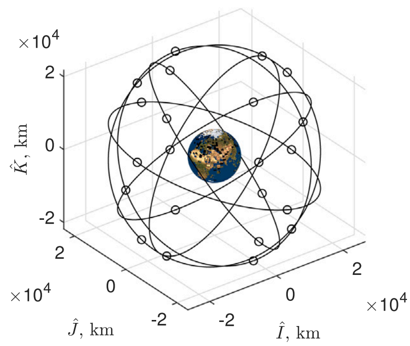

(a) GPS constellation.

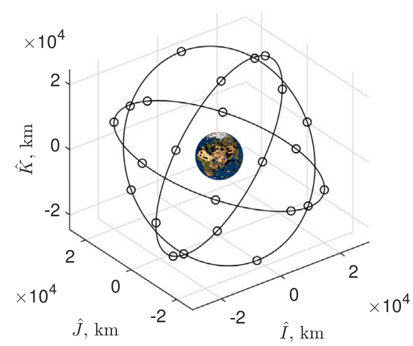

(b) Galileo constellation.

Fig. 5. Configurations of the GPS and Galileo constellations.

Table 4
Geometrical information of the Iridium constellation.

Parameter	Symbol	Value
Number of satellites	N	66
Number of orbital planes	P	6
Number of satellites per orbital plane	S	11
Inclination	i	86.4 deg
Altitude	h	780 km
RAAN spacing for co-rotating interface	$\Delta\Omega_{co}$	31.6 deg
RAAN spacing for counter-rotating interface	$\Delta\Omega_{counter}$	158.0 deg
Intra-plane AoL spacing	Δu_{intra}	32.7 deg
Inter-plane AoL spacing	Δu_{inter}	14.3 deg
Central angle of coverage	ϑ	20.0 deg
Angular radius of the footprint	θ	22.4 deg

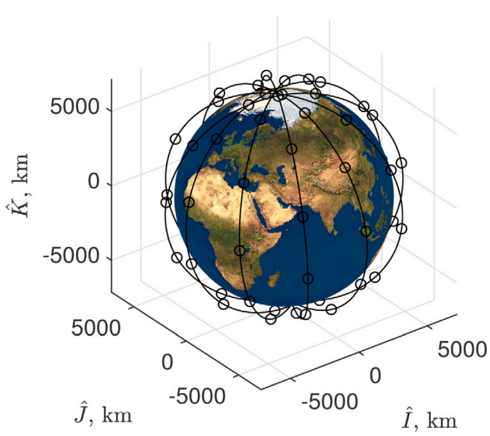

Fig. 6. Configuration of the Iridium constellation.

4. Constellation property assessment and trade-off analysis

In this section, seven constellation properties reported in Table 1 will be quantitatively assessed using the characteristic parameters identified in Section 3, and the trade-offs between properties will be analysed.

4.1. Coverage

Traditionally, the coverage performance is the prime criterion for constellation design since coverage is the original motive that constellations were created [1, page 674]. Here the coverage performance refers to whether the required coverage is provided and how efficient it is. For continuous global coverage Walker and SoC constellations, the required coverage can be guaranteed if the altitude is higher than the lower bound given in Eq. (13). So the coverage property to be discussed in the followings is the coverage efficiency.

A common approach to assessing the coverage efficiency for continuous global coverage constellations is the excess coverage, cov, which evaluates the total coverage available as a percentage of the total coverage required [1, page 726]. Here, the total coverage required is the area of the Earth's surface multiplied by the required coverage fold, and for a circular-orbit constellation in which all satellites are placed at the same altitude, the total coverage available is the area of a single footprint multiplied by the number of satellites. cov is given by [1, page 726]

$$cov = \frac{N \times 2\pi R_{\oplus}^2 (1-\cos\theta)}{4\pi R_{\oplus}^2 \times j} = \frac{N(1-\cos\theta)}{2j} \tag{14}$$

where θ can be derived from h using Eq. (12) and a given ϵ.

A small excess coverage indicates small coverage overlaps and low redundancy of satellite utility, hence high coverage efficiency. Thus, the lower the value of cov, the higher the coverage efficiency will be. From Eq. (14), the coverage efficiency can be improved by decreasing the number of satellites and altitude, as θ is directly linked to h, if ϵ is fixed.

For a particular i: $N/P/F$ Walker or i: N/P SoC constellation, the highest coverage efficiency achievable is represented by the minimum value of cov, denoted by $cov_{\min}$. $cov_{\min}$ is obtained by setting $\theta = \vartheta$, i.e.:

$$cov_{\min} = \min_{\theta} cov = \frac{N(1-\cos\vartheta)}{2j} \tag{15}$$

recalling that the central angle of coverage is the minimum angular radius of the footprint required for a specified fold of continuous global coverage. In other words, one can always link $cov_{\min}$ to ϑ, and analogous to ϑ, $cov_{\min}$ is independent of h but can be determined if N, P, F (Walker only), and i are known. Moreover, $cov_{\min}$ also sets the lower bound for cov, i.e.:

$$cov \geq cov_{lb} := cov_{\min} \tag{16}$$

If a constellation's cov_{lb} is too high, then the constellation can already be excluded from the optimal design because it will not be able to achieve a good enough coverage efficiency.

Fig. 7 shows the highest coverage efficiency achievable by Walker and SoC constellations for given numbers of satellites, for 1- and 4-fold continuous global coverage. In the plots, each point represents a class of coverage-optimal constellations sharing a particular set of N, P, F (Walker only), and i, whose $cov_{\min}$ is smaller than all other similar constellations with the same N, and accordingly, the y-axis represents the smallest $cov_{\min}$ for a given N.

As shown in Fig. 7, for a given N, the highest coverage efficiency achievable by the Walker constellation is always better than that by the SoC constellation, apart from some cases when $N \geq 20$ for 1-fold continuous global coverage. One possible reason is that for the SoC

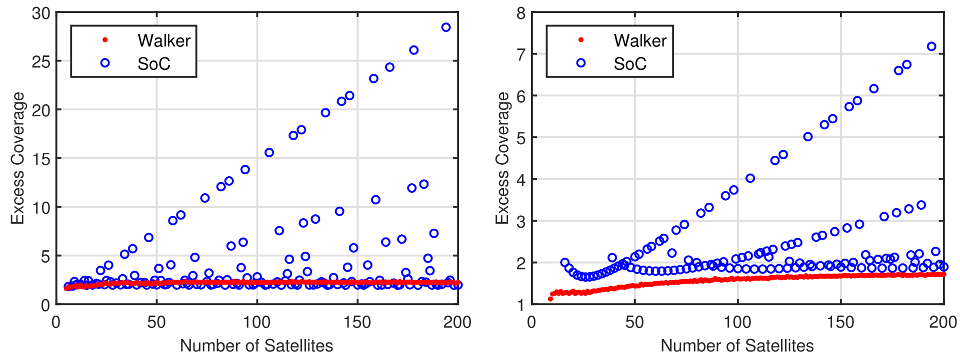

(a) 1-fold continuous global coverage. **(b) 4-fold continuous global coverage.**

Fig. 7. Highest coverage efficiency achievable by Walker and SoC constellations for given numbers of satellites (dot: Walker, circle: SoC).

constellation, as demonstrated by Eq. (11), there exists a constraint on the number of orbital planes. Taking as example a constellation with 66 satellites, the Walker constellation can have 66 orbital planes, while the SoC constellation can have at most six orbital planes. If we fix the number of orbital planes as a relatively small value, e.g. $P = 6$, the SoC constellation will be able to achieve better highest coverage efficiency than the Walker constellation, as shown in Fig. 8, which is consistent with the SoC constellation's advantage in terms of the coverage overlap. In the plots, each point represents a class of coverage-optimal constellations sharing a particular set of N, P (here $P = 6$), F (Walker only), and i, whose $cov_{\min}$ is smaller than all other similar constellations with the same N and P, and accordingly, the y-axis represents the smallest $cov_{\min}$ for given N and P.

It is of note that, although the coverage performance is a principle design criterion, the coverage-optimal constellations may not suit practical applications. Here are the reasons.

(1) Most of the coverage-optimal Walker constellations in Fig. 7 are characterised by $P = N$, whose central angles of coverage are smaller than those of the similar constellations with the same numbers of satellites, as shown in Fig. 3. However, such constellations may lead to a high self-induced collision risk and a long build-up period; a demonstration of this concept will be given in Sections 4.3 and 4.5.
(2) All the coverage-optimal SoC constellations in Figs. 7 and 8 are characterised by $i = 90$ deg, whose central angles of coverage are smaller than those of the similar inclined constellations with the same numbers of satellites and orbital planes [8]. However, such constellations will lead to a high self-induced collision risk and a high launch cost; a demonstration of this concept will be given in Sections 4.3 and 4.4.

In the following sections we will show the other properties for the coverage-optimal constellations, to demonstrate the need of performing trade-off during constellation design.

4.2. Robustness

In this study, the robustness property is defined as the constellation performance to offer normal services, should one satellite fail. It is assessed by the average percentage of the Earth's surface visible to $(j + 1)$ satellites over one orbit period, denoted by pct, where j is the required coverage fold. The physical meaning of pct is that once a satellite fails and no matter which one it is, there will be pct-percent of the Earth's surface visible to at least j satellites, i.e., the required j-fold continuous global coverage can be maintained over pct-percent of the Earth's surface. Thus, the higher the value of pct, the stronger the robustness will be.

The logic flow to compute pct is as follows.

(1) Generating a set of test points on the Earth's surface.
(2) Computing the locations of sub-satellite points at small time steps in one orbit period.
(3) Computing the number of test points enclosed by at least $(j + 1)$ footprint circles as the percentage of the total number of test points at each time step.
(4) Averaging the percentages over all time steps in one orbit period.

pct is a function of the characteristic parameters, the number of test points, and the size of time step; the more the test points and the shorter the time step, the more accurate pct will be.

Fig. 9 shows the robustness of the coverage-optimal Walker and SoC constellations for given numbers of satellites at their lowest allowable altitudes, for 1- and 4-fold continuous global coverage, with the y-axis representing the value of pct. Here the lowest allowable altitude is the altitude's lower bound given by Eq. (13), assuming $\epsilon = 5$ deg. In the computation, the test points are selected along latitudes and longitudes at intervals of 1 deg, and the time step is set to $T/10^3$, where

$$T = 2\pi\sqrt{\frac{(h + R_{\oplus})^3}{\mu}} \tag{17}$$

is the unperturbed orbit period, with $\mu \approx 3.9860\times10^5$ km^3/s^2 being the Earth gravitational parameter.

Intuitively, the robustness property, which would benefit from large coverage overlaps and high redundancy of satellite utility, should be in contrast with the coverage property. However, comparing Fig. 9 with Fig. 7, it is observed that these two properties are not completely contrary with each other. Particularly, for 4-fold continuous global coverage, the coverage-optimal SoC constellations do not always show a stronger robustness than the coverage-optimal Walker constellations at their lowest allowable altitudes. One possible reason is due to the SoC constellation's design logic; the minimised coverage overlap on the co-rotating interface will lead to a larger area of outage.

By widely checking different combinations of characteristic parameters, we find that the robustness can be enhanced by increasing the number of satellites and orbital planes, increasing the altitude, using a medium inclination for the Walker constellation, and increasing the inclination for the SoC constellation.

4.3. Self-induced collision avoidance

As the outer space is becoming more and more densely populated by satellites, collision avoidance is a critical issue that must be taken into consideration at the design stage. In this study we focus on the self-induced collision caused by satellites from the same constellation. If one collision happens within a constellation, it will be of high possibility to trigger a chain reaction, not only destroying the constellation itself but also posing severe safety hazards to the other operational

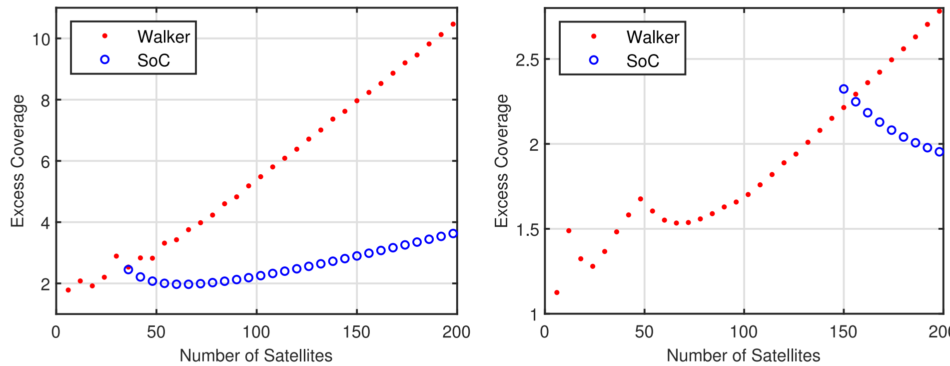

(a) 1-fold continuous global coverage. **(b) 4-fold continuous global coverage.**

Fig. 8. Highest coverage efficiency achievable by Walker and SoC constellations consisting of six orbital planes for given numbers of satellites (dot: Walker, circle: SoC).

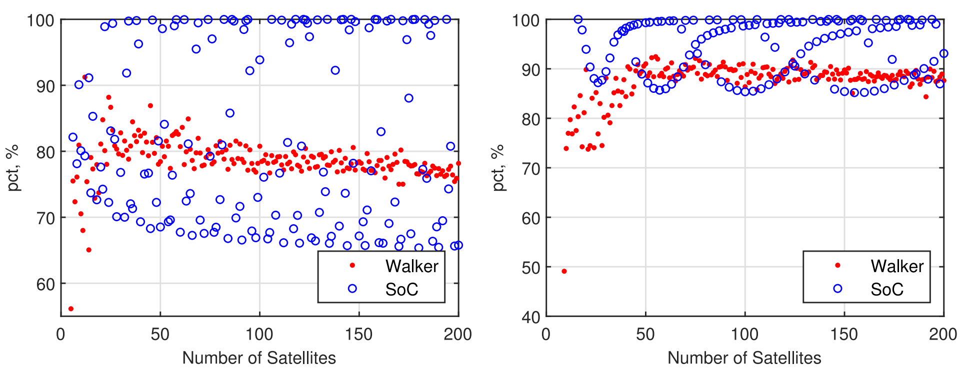

(a) 1-fold continuous global coverage. **(b) 4-fold continuous global coverage.**

Fig. 9. Robustness of the coverage-optimal Walker and SoC constellations for given numbers of satellites at lowest allowable altitudes (dot: Walker, circle: SoC).

spacecraft. In this study, the self-induced collision avoidance property is defined as the constellation performance to avoid collision without performing any manoeuvre. It is assessed from two aspects: the collision opportunity and the miss distance.

4.3.1. Collision opportunity

In Ref. [1, page 709], the collision opportunity was defined as an incident where two satellites may approach each other within a distance lower than the sum of the radii of these two satellites. Supposing satellite A and satellite B in different orbital planes, satellite A passes through the plane of satellite B twice per revolution, and so does satellite B. Thus, each satellite in a constellation consisting of P orbital planes passes through the other planes $2(P-1)$ times per revolution. For a constellation with N satellites and P orbital planes, it will have $2N(P-1)$ collision opportunities per revolution. Take as example the Iridium constellation having 66 satellites and 6 orbital planes with approximately 14.3 revolutions per day. In a 10-year-lifetime, the Iridium constellation has 3.5×10^7 collision opportunities. If a less than 1% collision probability in 10 years is desired, then the probability of a collision in any single opportunity should be less than 10^{-9}, and even less than 10^{-11}, considering the catastrophic consequence of a collision [1, page 710].

In this study we introduce a unit collision opportunity, opp, to evaluate the collision opportunities per unit time. It is defined by

$$opp = \frac{2N(P-1)}{T} = \frac{\sqrt{\mu}}{\pi}\frac{N(P-1)}{(h+R_{\oplus})^{3/2}} \tag{18}$$

Apparently, the lower the value of opp, the better the constellation performance to avoid self-induced collision. From Eq. (18), the unit collision opportunity can be reduced by decreasing the number of satellites and orbital planes, and by increasing the altitude.

4.3.2. Miss distance

In Ref. [14], the miss distance, ψ, was defined as the minimum angular separation between a pair of satellites. Speckman et al. [35] derived the analytical solution of ψ for circular-orbit constellations in which all satellites are placed at the same altitude and inclination:

$$\cos\psi = \cos^2\alpha - \sin^2\alpha\cos\beta \tag{19}$$

where

$$\alpha = \Delta u_{s/c}/2 + \tan^{-1}\left[\tan\left(\Delta\Omega_{s/c}/2\right)\cos i\right] \tag{20a}$$

$$\cos\beta = \cos^2 i + \sin^2 i\cos\Delta\Omega_{s/c} \tag{20b}$$

with $\Delta\Omega_{s/c}$ and $\Delta u_{s/c}$ being the relative RAAN and AoL, respectively, between a pair of satellites.

In this study we introduce the constellation miss distance, Ψ, to assess the constellation as a whole. It is the minimum value of ψ for all pairs of satellites of a constellation, given by

$$\Psi = \min_{A,\,B}\psi_{AB} \tag{21}$$

where ψ_{AB} is the miss distance between the Ath and Bth satellites, with $1 \le A \le N$, $1 \le B \le N$, and $A \ne B$. Apparently, the larger the constellation miss distance, the better the constellation performance to avoid self-induced collision.

Figs. 10 and 11 show the constellation miss distances of the coverage-optimal Walker and SoC constellations, respectively, for given numbers of satellites and orbital planes, for 1- and 4-fold coverage. In the plots, the constellations having a zero Ψ are highlighted with red dots.

As shown in the figures, the constellation miss distance generally decreases with the number of satellites and orbital planes. Especially, for the coverage-optimal SoC constellations, i.e., the polar ones, that

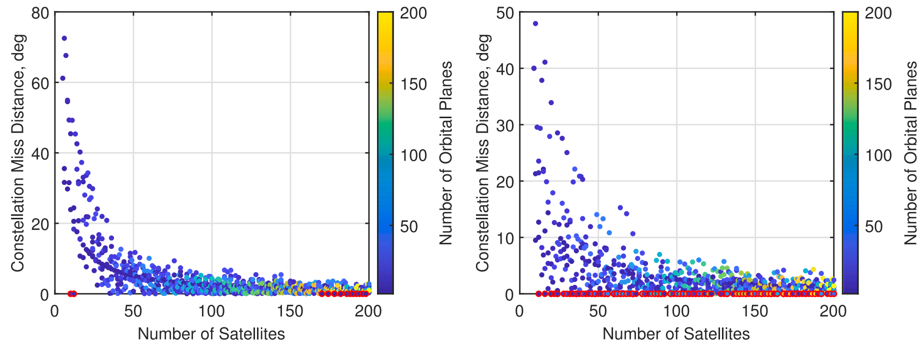

(a) 1-fold continuous global coverage.

(b) 4-fold continuous global coverage.

Fig. 10. Constellation miss distances of the coverage-optimal Walker constellations for given numbers of satellites and orbital planes (the number of orbital planes increasing as the colour from dark to light).

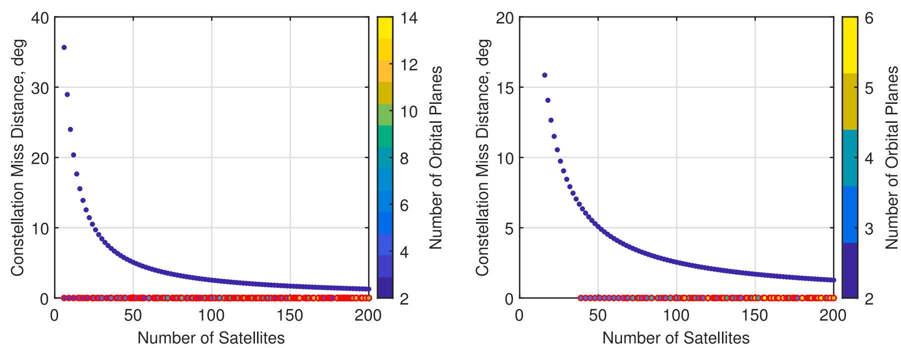

(a) 1-fold continuous global coverage.

(b) 4-fold continuous global coverage.

Fig. 11. Constellation miss distances of the coverage-optimal SoC constellations for given numbers of satellites and orbital planes (the number of orbital planes increasing as the colour from dark to light).

have more than two orbital planes, collision will definitely happen at the poles because the satellite distribution will repeat itself every other orbital plane. This is the reason why the polar SoC constellation cannot be used for practical applications.

4.4. Launch

In this study, the launch property is defined as the launch cost to deliver the constellation into the mission orbit by an arbitrary launcher. Generally speaking, there are two approaches to delivering a spacecraft to the mission orbit: the direct injection and the indirect injection [36, Sec. 18.2]. The direct injection is such that the spacecraft is directly injected into the mission orbit by the launcher. The indirect injection is such that the spacecraft is first injected into a parking orbit by the launcher and then sent to the mission orbit either by the launcher's upper stage or by the spacecraft on-board propulsion system.

As summarised in Ref. [1, Table 13-2], the launch cost is determined by three factors: altitude, inclination, and spacecraft mass. For a general study of constellation design, the spacecraft mass can be replaced by the number of satellites of a constellation, the latter representing the total payload weight to launch. In the following we will present two indexes to assess the launch cost.

For direct injection, the launch cost can be assessed by the total Δv-budget of all satellites of a constellation, because it represents the total amount of fuel required. For indirect injection, the Δv-budget is affected by the parking orbit, and thus there does not exist a general formula to evaluate the Δv-budget. As a study focused on the design of constellation configuration, the selection of parking orbit will not be specifically discussed because it depends on the mission requirement and the system design of launcher and satellite. Nonetheless, due to the fact that the Δv-budget is proportional, although not strictly, to the number of satellites and altitude, here we propose

$$lch_h = Nh \tag{22}$$

as one index to assess the launch cost. lch_h is consistent with the principle option for constellation design reported in Ref. [1, Table 13-2], in terms of reducing the launch cost.

For the purpose of employing the Earth's rotation effects, the inclination of a prograde-orbit (i.e. $i \leq 90$ deg) constellation must not be smaller than the latitude of the launch site ϕ_{site} [36, Sec. 6.4]. Moreover, the higher the inclination, the less the launch benefits from the Earth's rotation effects, because the velocity gained by the Earth's rotation effects is $v = v_{\oplus} \cos i$, where $v_{\oplus} \approx 464.5$ m/s is the velocity of the Earth's rotation at the equator [36, Sec. 6.4]. From the aforementioned reasons, Ref. [14] inferred that the launcher's payload capability decreases as the inclination increases above the latitude of the launch site, where the launcher's payload capability refers to the launcher's capability to boost a necessary amount of payloads to the mission orbit [36, Sec. 18.2]; a low difference between i and ϕ_{site} will allow a large margin for the amount of payloads. Therefore, we propose

$$lch_i = i - \phi_{\text{site}} \tag{23}$$

as another index to assess the launch cost. lch_i is a monotonically decreasing function of the velocity gained by the Earth's rotation effect.

Fig. 12 shows the inclinations of the coverage-optimal Walker constellations for given numbers of satellites, for 1- and 4-fold continuous global coverage. It is observed that in most cases the inclinations of the coverage-optimal Walker constellations is relatively high, indicating that if the launch site is at a low latitude, a good coverage property will lead to a bad launch property. This implies the need to perform a trade-off between the coverage and launch properties when selecting the

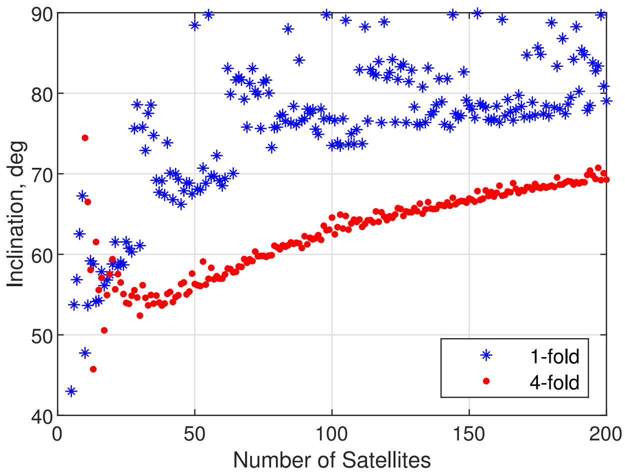

Fig. 12. Inclinations of the coverage-optimal Walker constellations for given numbers of satellites, for 1- and 4-fold continuous global coverage (asterisk: 1-fold, dot: 4-fold).

inclination. For the SoC constellation, such trade-off is also necessary because the coverage-optimal SoC constellations are always the polar ones.

From Eqs. (22) and (23), the launch cost can be reduced by decreasing the number of satellites, altitude, and inclination. Note that, although in this section some simplifications are introduced, they would be necessary and useful by providing a simplified version of a complicated topic.

4.5. Build-up

Due to the long duration from the testing of the early-launched satellites to the launching of all satellites, a constellation may spend a great part of its lifetime in an incomplete configuration [1, page 718]. If the build-up process is very slow, the early-launched satellites may become non-operational in orbit before the expected performances are achieved. In this case, the spares will have to be launched to take over the non-operational satellites, increasing the system cost and the difficulty of orbit operation. Thus, the period of building up a full constellation is an important cost driver. In this study, the build-up property is defined as the build-up period.

In real missions, the detailed process of building up a full constellation is unique and strongly related to the launch system, i.e., the choice of launcher, the number of satellites that can be placed in orbit by a single launch, etc. [1, page 719] Recalling that this is a general study focused on the design of constellation configuration, the launch system will not be specifically discussed. If irrespective of the launch system, the build-up period can be considered an increasing function of the number of orbital planes.

So far, the technology of injecting multiple satellites into a single orbital plane is mature. For example, India has successfully launched 104 satellites at once in February 2017 [37]. Without loss of generality, suppose that the orbital planes are built up one by one and there is no limit on the number of satellites by a single launch nor the time interval of launch. Then the number of orbital planes can be used to evaluate the build-up period; the less the orbital planes, the better the build-up property will be. The following index is proposed:

$$bld = P \tag{24}$$

4.6. Station-keeping

In this study, the station-keeping property is defined as the cost to maintain the overall constellation configuration. The major purpose of station-keeping for constellations is to allow normal services provided and to avoid self-induced collision [1, Sec. 13.4]. Generally speaking, there are two alternative approaches to station-keeping [1, Sec. 13.4]. One is the absolute station-keeping by maintaining the absolute position of a satellite within a predefined station-keeping box. The other is the relative station-keeping by maintaining the relative positions of satellites with respect to each other. The station-keeping for constellations belongs to the latter approach [1, Sec. 13.4]. In this study we consider the J_2 and drag effects only. Because all satellites of a Walker or SoC constellation are placed in circular orbits at the common altitude and inclination, the secular rates of nodal regression and apsidal procession due to J_2 are the same for every satellite. In this case the only parameter that needs to be maintained is the altitude, which will decay under the drag effect. Thus, the station-keeping cost can be quantitatively assessed by the cost of altitude maintenance, which in turn can be evaluated in terms of the total Δv-budget of all satellites of the constellation. It is important to multiply the Δv-budget of a single satellite by the total number of satellites, because the total Δv-budget is proportional to the total amount of fuel carried by all satellites, which is proportional to the mass carried by the launcher and, as a result, affects the launch cost. Note that the altitude maintenance is required only by the constellations in LEO, where the drag effect cannot be neglected.

Supposing the altitude maintenance can be achieved via a 2-burn Hohmann transfer, the total Δv-budget is given by

$$\Delta v_{\text{keep}} = N\left[\left(\sqrt{\frac{2\mu}{a_f} - \frac{2\mu}{a_n + a_f}} - \sqrt{\frac{\mu}{a_f}}\right) + \left(\sqrt{\frac{\mu}{a_n}} - \sqrt{\frac{2\mu}{a_n} - \frac{2\mu}{a_n + a_f}}\right)\right] \tag{25}$$

where a_n is the semi-major axis of the nominal orbit, a_f is the final semi-major axis after altitude decay. a_f can be obtained by integrating the differential equation [38, page 525–529]

$$\frac{\mathrm{d}a}{\mathrm{d}t} = -\frac{C_D A}{m}\rho\sqrt{\mu a} \tag{26}$$

where $m/C_D A$ is the ballistic coefficient, ρ is the atmospheric density, given by the exponential model

$$\rho = \rho^* \exp\left(-\frac{a - a^*}{h_s}\right) \tag{27}$$

with ρ^* being the reference atmospheric density, a^* being the reference semi-major axis, and h_s being the scale height.

For a fixed frequency of altitude maintenance operation, the lower the value of Δv_{keep}, the lower the station-keeping cost will be. From Eq. (25), the station-keeping cost can be reduced by decreasing the number of satellites and by increasing the altitude, because the drag effect is weak at high altitudes.

4.7. End-of-life disposal

In this study, the EoL disposal property is defined as the cost to remove the constellation from the nominal orbit. According to the international regulation, non-operational spacecraft must be removed from the nominal orbit after end of life. Specifically, spacecraft in LEO should be de-orbited to a disposal orbit with low enough perigee so as to quickly re-enter under the drag effect, while spacecraft in MEO should be raised to a graveyard orbit higher than the nominal one so as not to interfere with other operational spacecraft [1, page 723]. As a matter of fact, a MEO constellation can also re-enter to the Earth if all satellites of the constellation are equipped with passive de-orbiting devices (e.g. solar/drag sail) and moved to the condition of orbital resonances that can provoke rapid orbital decay [39,40]. However, we consider here the graveyard orbit strategy for the purpose of carrying out a general study of constellation design. Analogous to station-keeping, the EoL disposal cost is also quantitatively evaluated in terms of the total Δv-budget of all satellites of the constellation.

Table 5
Influence of the characteristic parameters on the constellation properties.

Property	Index	N	P	h	i	
					Walker	SoC
Coverage	cov	↓	–	↓	–	–
Robustness	pct	↑	↑	↑	Medium	↑
Self-induced collision avoidance	opp	↓	↓	↑	–	–
Self-induced collision avoidance	Ψ	↓	↓	–	–	$\neq 90\ deg\,(P>2)$
Launch	lch_h	↓	–	↓	–	–
Launch	lch_i	–	–	–	↓	↓
Build-up	bld	–	↓	–	–	–
Station-keeping	Δv_{keep}	↓	–	↑	–	–
EoL disposal for LEO constellations	$(\Delta v_{\mathrm{eol}})_{\mathrm{LEO}}$	↓	–	↓	–	–
EoL disposal for MEO constellations	$(\Delta v_{\mathrm{eol}})_{\mathrm{MEO}}$	↓	–	↑	–	–

For LEO constellations, supposing the de-orbiting can be achieved via a tangential burn, the total Δv-budget is given by

$$(\Delta v_{\mathrm{eol}})_{\mathrm{LEO}} = N\left(\sqrt{\frac{\mu}{a_n}} - \sqrt{\frac{2\mu}{a_n} - \frac{2\mu}{a_n + r_{pd}}}\right) \tag{28}$$

where $r_{pd} = h_{pd} + R_\oplus$ is the perigee radius of the disposal orbit, with h_{pd} being the perigee altitude; lower than h_{pd} the drag will be strong enough to quickly lower the apogee and lead to re-entry.

For MEO constellations, supposing the orbit raising can be achieved via a 2-burn Hohmann transfer, the total Δv-budget is given by

$$(\Delta v_{\mathrm{eol}})_{\mathrm{MEO}} = N\left[\left(\sqrt{\frac{2\mu}{a_g} - \frac{2\mu}{a_n + a_g}} - \sqrt{\frac{\mu}{a_g}}\right) + \left(\sqrt{\frac{\mu}{a_n}} - \sqrt{\frac{2\mu}{a_n} - \frac{2\mu}{a_n + a_g}}\right)\right] \tag{29}$$

where a_g is the semi-major axis of the graveyard orbit.

Apparently, the smaller the total Δv-budget, the lower the EoL disposal cost will be. From Eq. (28), for a given disposal perigee altitude, the EoL disposal cost for LEO constellations can be reduced by decreasing the number of satellites and altitude. From Eq. (29), for a given semi-major axis increment, the EoL disposal cost for MEO constellations can be reduced by decreasing the number of satellites and by increasing the altitude.

4.8. Trade-off analysis

Table 5 summarises the influence of the characteristic parameters on the constellation properties. In the table, the up and down arrows indicate that the properties benefit from increasing and decreasing, respectively, the characteristic parameters, whereas the symbol "–" indicates that the characteristic parameters do not show explicit impacts on the properties, if using the assessment methods proposed. Note that for the Walker constellation, the robustness property can be enhanced by using medium inclination, and for the SoC constellation, the inclination must not be 90 deg if there are more than two orbital planes, otherwise collision will happen.

Some conclusions can be drawn from the table.

(1) There are trade-offs between the robustness property and the other properties in terms of the number of satellites and orbital planes, i.e., the other properties benefit from small N and P while the robustness property benefit from large N and P.
(2) There are trade-offs between properties in terms of the altitude, e.g., between coverage and robustness properties, between robustness and launch property, between launch and station-keeping properties, etc.
(3) There is a trade-off between the robustness and launch properties in terms of the inclination.

5. Multi-objective optimisation for constellation design

In this section we will find the globally optimal constellations for given missions by taking the seven constellation properties investigated in Section 4 into consideration. A multi-objective global optimiser will be used to search for the Pareto-front solutions through a multi-agent-based search approach hybridised with a domain decomposition technique [41].

5.1. Mission scenarios

Two different missions are considered: a 1-fold LEO mission and a 4-fold MEO mission; the former is usually used for Earth's observation or telecommunications (e.g. the Iridium constellation), and the latter can be applied to navigation and positioning (e.g. the GPS and Galileo constellations). For both missions, the elevation angle is fixed as $\epsilon = 10$ deg, and the latitude of the launch site is set to $\phi_{\mathrm{site}} = 6$ deg. It is assumed that the altitude maintenance for the LEO mission is performed once per year, and the ballistic coefficient is set to $m/C_D A = 83.33$ kg/m^2 for all satellites. Concerning the EoL disposal, the LEO mission will be de-orbited to a disposal perigee altitude of $h_{pd} = 250$ km, lower than which satellites can quickly re-enter due to the drag effect, whereas the MEO mission will be moved to a graveyard altitude which is 500 km higher than the nominal one.

5.2. Design variables

In this study, the design variables are simply the characteristic parameters given by Table 2, and the design variable vectors for Walker and SoC constellations are therefore

$$\boldsymbol{x}_{\mathrm{Walker}} = \{N,\ P,\ F, h,\ i\}^\top \tag{30a}$$

$$\boldsymbol{x}_{\mathrm{SoC}} = \{N,\ P,\ \ h,\ i\ \}^\top \tag{30b}$$

Table 6 gives the bounds for the design variables, where the lower bound for N indicates the minimum number of satellites that can offer the required fold of continuous global coverage within the given altitude range. Besides, there are also some other constraints on the design variables.

(1) P should be an integer divisor of N. For the SoC constellation, P should also satisfy Eq. (11).
(2) For the Walker constellation, F should be an integer between 0 and $(P-1)$.
(3) h should be higher than the lower bound given by Eq. (13), where the central angle of coverage ϑ, which is determined by the design variables, must be less than 90 deg.
(4) The design variables that lead to a zero constellation miss distance should be excluded.

Table 6
Bounds for the design variables.

Constellation	Parameter	Symbol	Bound			
			1-fold LEO mission		4-fold MEO mission	
			Lower	Upper	Lower	Upper
Walker	Number of satellites	N	30	200	15	200
SoC	Number of satellites	N	28	200	22	200
Walker, SoC	Inclination	i	ϕ_{site}	$\pi/2$ rad	ϕ_{site}	$\pi/2$ rad
Walker, SoC	Altitude	h	600 km	2000 km	2000 km	35786 km

5.3. Objective functions

In this multi-objective optimisation problem, each of the seven constellation properties is to be modelled as an objective function and then minimised. The objective functions are defined as follows.

$$J_1 = cov \tag{31a}$$

$$J_2 = -\frac{pct}{10} \tag{31b}$$

$$J_3 = \frac{\log\left(\frac{\pi}{\sqrt{\mu}} opp_{ub}\right) - \log\left(\frac{\pi}{\sqrt{\mu}} opp_{\text{lb}}\right)}{\log\left(\frac{\pi}{\sqrt{\mu}} opp_{\text{ub}}\right) - \log\left(\frac{\pi}{\sqrt{\mu}} opp_{\text{lb}}\right)} + \frac{\frac{\pi}{2} - \Psi}{\frac{\pi}{2}} \tag{31c}$$

$$J_4 = \frac{\log\left(lch_h\right)_{ub} - \log\left(lch_h\right)_{\text{lb}}}{\log\left(lch_h\right)_{\text{ub}} - \log\left(lch_h\right)_{\text{lb}}} + \frac{i - \phi_{\text{site}}}{\frac{\pi}{2} - \phi_{\text{site}}} \tag{31d}$$

$$J_5 = bld \tag{31e}$$

$$J_6 = \log \Delta v_{\text{keep}} \tag{31f}$$

$$\left(J_7\right)_{\text{LEO}} = \log\left(\Delta v_{\text{eol}}\right)_{\text{LEO}}, \quad \left(J_7\right)_{\text{MEO}} = \log\left(\Delta v_{\text{eol}}\right)_{\text{MEO}} \tag{31g}$$

where J_1, J_2, J_3, J_4, J_5, and J_6 are the objective functions of the coverage, robustness, self-induced collision avoidance, launch, build-up, and station-keeping properties, respectively, $\left(J_7\right)_{\text{LEO}}$ and $\left(J_7\right)_{\text{MEO}}$ are the objective functions of the EoL disposal property for the LEO and MEO missions, respectively. In Eqs. (31c) and (31d), the subscripts lb and ub represent the lower and upper bounds, respectively, for opp and lch_h, which are given by the means of

$$opp_{\text{lb}} = \frac{\sqrt{\mu}}{\pi}\frac{\min\left[N\left(P-1\right)\right]}{\left(2000 + R_{\oplus}\right)^{3/2}}, \quad opp_{\text{ub}} = \frac{\sqrt{\mu}}{\pi}\frac{\max\left[N\left(P-1\right)\right]}{\left(600 + R_{\oplus}\right)^{3/2}}$$
$$\left(lch_h\right)_{\text{lb}} = \left(\min N\right)\times 600, \quad \left(lch_h\right)_{\text{ub}} = \left(\max N\right)\times 2000 \tag{32}$$

for the 1-fold LEO mission, and

$$opp_{\text{lb}} = \frac{\min\left[N\left(P-1\right)\right]}{\left(35786 + R_{\oplus}\right)^{3/2}}, \quad opp_{\text{ub}} = \frac{\max\left[N\left(P-1\right)\right]}{\left(2000 + R_{\oplus}\right)^{3/2}}$$
$$\left(lch_h\right)_{\text{lb}} = \left(\min N\right)\times 2000, \quad \left(lch_h\right)_{\text{ub}} = \left(\max N\right)\times 35786 \tag{33}$$

for the 4-fold MEO mission; the minimum and maximum values of $N\left(P-1\right)$ and N can be obtained based on the bounds for the design variables given in Section 5.2.

The rationale behind the definitions of the objective functions is explained as follows.

(1) All the properties are optimised by minimising their respective objective functions. Recall that the properties refer to performances or costs, where the performances are to be maximised and the costs are to be minimised. For the performances which are improved by increasing the corresponding indexes, a minus sign should be accordingly added. In Eqs. (31b) and (31c), the robustness and self-induced collision avoidance properties are improved by increasing the indexes pct and Ψ, so a minus sign is added to these two indexes.

(2) For the self-induced collision avoidance and launch properties, each of them is assessed by two different indexes, and the two indexes should be properly scaled according to their respective lower and upper bounds such that they can be formulated together as a single objective. To be specific:
- the lower and upper bounds for opp and lch_h are given by Eqs. (32) and (33);
- the lower and upper bounds for i are given in Table 6;
- the lower and upper bounds for Ψ are 0 and $\pi/2$ rad, respectively.

(3) For the indexes related to h, i.e., opp, lch_h, Δv_{keep}, $(\Delta v_{\text{eol}})_{\text{LEO}}$, and $(\Delta v_{\text{eol}})_{\text{MEO}}$, their values may vary from 10^{-4} to 10^{6}. In order to reduce the impact by h and to enhance the convergence of the optimisation process, the base 10 logarithm is therefore used.

Finally, the objective vectors for the LEO and MEO missions are

$$\boldsymbol{J}_{\text{LEO}} = \left\{J_1,\ J_2,\ J_3,\ J_4,\ J_5,\ J_6,\ \left(J_7\right)_{\text{LEO}}\right\}^{\top} \tag{34a}$$

$$\boldsymbol{J}_{\text{MEO}} = \left\{J_1,\ J_2,\ J_3,\ J_4,\ J_5,\ \left(J_7\right)_{\text{MEO}}\right\}^{\top} \tag{34b}$$

Note that $\boldsymbol{J}_{\text{MEO}}$ does not include J_6 because the altitude maintenance is required only by LEO constellations.

5.4. Results and discussion

5.4.1. 1-fold LEO mission

Fig. 13 shows the Pareto-front solutions for the 1-fold LEO mission, each point representing an optimal constellation. In the plots, the three axes indicate the number of satellites, the inclination, and the altitude, and the colour bar indicates the number of orbital planes.

As presented in Section 4.8, there exist various trade-offs between properties, and these trade-offs are also demonstrated here by the multi-objective optimisation results. Fig. 14 shows as example two pairs of objectives: J_1 versus J_2 and J_6 versus $\left(J_7\right)_{\text{LEO}}$, corresponding to the trade-off between the coverage and robustness properties and the trade-off between the station-keeping and EoL disposal properties. It can be seen that the different objectives do weigh against each other depending on their dimensions and scaling, and a small increase in one objective will lead to a decrease in the other objective, and vice-versa.

Among the optimal constellations, we select two constellations at similar altitudes of the Iridium constellation as the alternatives to Iridium, and another two new constellations at altitudes between 1,200 and 1,400 km, where the space debris density is relatively low. In addition to the altitude constraints, the following issues should also be considered during the selection.

(1) The selected constellations should have relatively fewer satellites, as the number of satellites is traditionally the prime cost driver for small- and middle-sized constellations [1, Table 13-2];

(2) The selected constellations should have relatively larger constellation miss distance, considering the snowball effect which not only destroying the constellation itself but also posing severe safety threat to the other operational spacecraft in the already congested LEO region.

Table 7 presents the results of the Iridium constellation and of the selected optimal constellations. Some discussion about the results are as follows.

(1) Compared to the alternatives, the Iridium constellation shows excellent performances in terms of most of the properties apart

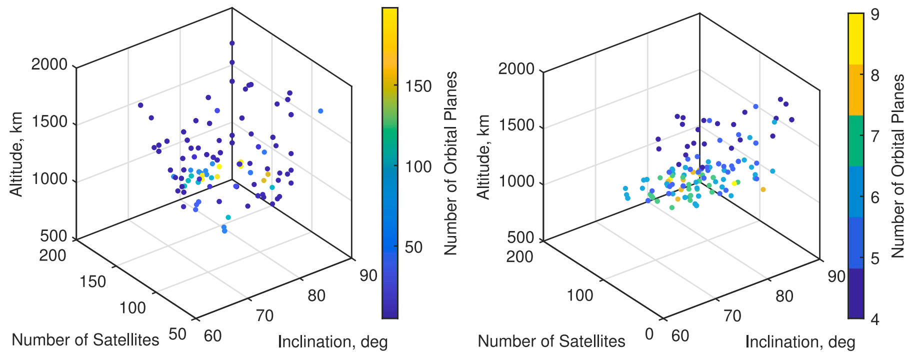

(a) Optimal Walker constellations. **(b) Optimal SoC constellations.**

Fig. 13. Pareto-front solutions for the 1-fold LEO mission (the number of orbital planes increasing as the colour from dark to light).

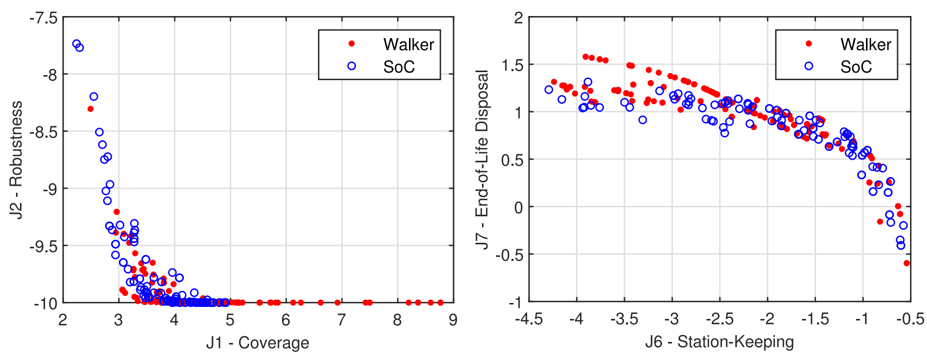

(a) J_1 versus J_2. **(b) J_6 versus $(J_7)_{LEO}$.**

Fig. 14. Sensitivity analysis of objectives for the 1-fold LEO mission (dot: Walker, circle: SoC).

from the robustness. For the Iridium constellation, once a satellite fails, on average only 57.72% of the Earth's surface can be offered with normal services. Considering that a replenishment operation will take some time, such an outage may cause a huge profit loss for both the ground users and the telecom operators. This represents a business trade-off that might not have been taken into account in the design of the Iridium constellation.

(2) Comparing the two new constellations, the SoC constellation is better than the Walker one in terms of most of the properties apart from the robustness. This is because the SoC constellation has fewer satellites and orbital planes, which, according to Table 5, benefits to all properties except the robustness.

Figs. 15 and 16 show the configurations of the selected optimal constellations for the 1-fold LEO mission in the ECI coordinate system, where the round markers and lines indicate the satellites and orbital planes, respectively.

5.4.2. 4-fold MEO mission

Fig. 17 shows the Pareto-front solutions for the 4-fold MEO mission, each point representing an optimal constellation. In the plots, the three axes indicate the number of satellites, the inclination, and the altitude, and the colour bar indicates the number of orbital planes. An interesting result is that all the optimal SoC constellations have only two orbital planes. One possible reason is that a high-altitude mission in MEO usually requires fewer satellites, while a 4-fold MEO mission with small number of satellites can lead to a high-demanding constraint on the number of orbital planes, as demonstrated by Eq. (11).

Fig. 18 shows as example two pairs of objectives: J_1 versus J_2 and J_1 versus $(J_7)_{MEO}$, corresponding to the trade-off between the coverage and robustness properties and the trade-off between the coverage and EoL disposal properties. It can be seen that the different objectives do weigh against each other depending on their dimensions and scaling, and a small increase in one objective will lead to a decrease in the other objective, and vice-versa.

Table 7
Results of the Iridium constellation and of the selected optimal constellations for the 1-fold LEO mission.

Symbol	Iridium	Alternative Iridium		New	
		Walker	SoC	Walker	SoC
N	66	126	126	72	48
P	6	7	7	24	6
F		3		8	
i, deg	86.4	87.0	79.6	77.2	82.4
h, km	780	776	773	1,321	1,286
J_1	1.74	3.29	3.27	3.46	2.24
J_2	−5.77	−9.57	−9.39	−10.00	−7.70
J_3	1.48	1.44	1.72	1.55	1.35
J_4	1.31	1.51	1.43	1.38	1.32
J_5	6	7	7	24	6
J_6	−2.00	−1.69	−1.67	−3.19	−3.31
$(J_7)_{LEO}$	0.50	0.77	0.76	1.11	0.91
cov	1.74	3.29	3.27	3.46	2.24
pct, %	57.72	95.69	93.91	99.95	77.05
opp, s^{-1}	0.11	0.25	0.25	0.49	0.07
Ψ, deg	0.30	1.89	0.58	0.29	0.76
lch_h, $\times 10^4$ km	5.15	9.78	9.73	9.51	6.17
lch_i, deg	80.40	80.98	73.64	71.21	76.43
bld	6	7	7	24	6
Δv_{keep}, m/s	10.10	20.33	21.23	0.64	0.49
$(\Delta v_{eol})_{LEO}$, km/s	3.16	5.89	5.76	12.89	8.20

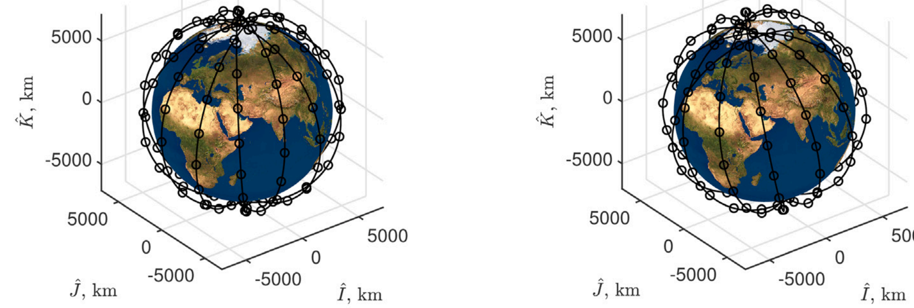

(a) Walker. **(b) SoC.**

Fig. 15. Alternatives to the Iridium constellation.

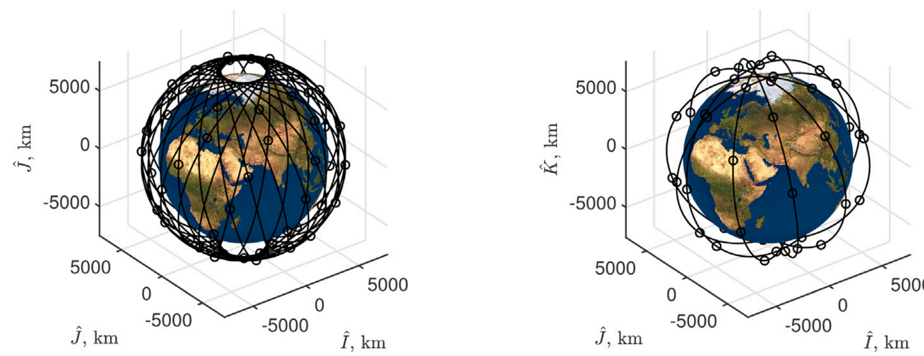

(a) Walker. **(b) SoC.**

Fig. 16. New constellations for the 1-fold LEO mission.

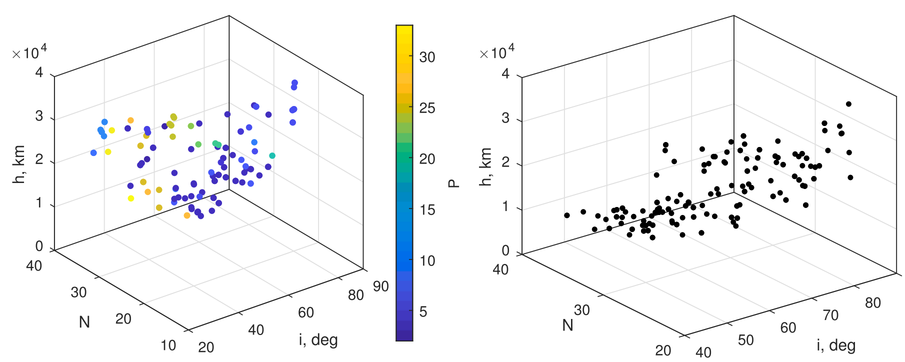

(a) Optimal Walker constellations. **(b) Optimal SoC constellations (two orbital planes).**

Fig. 17. Pareto-front solutions for the 4-fold MEO mission (the number of orbital planes increasing as the colour from dark to light).

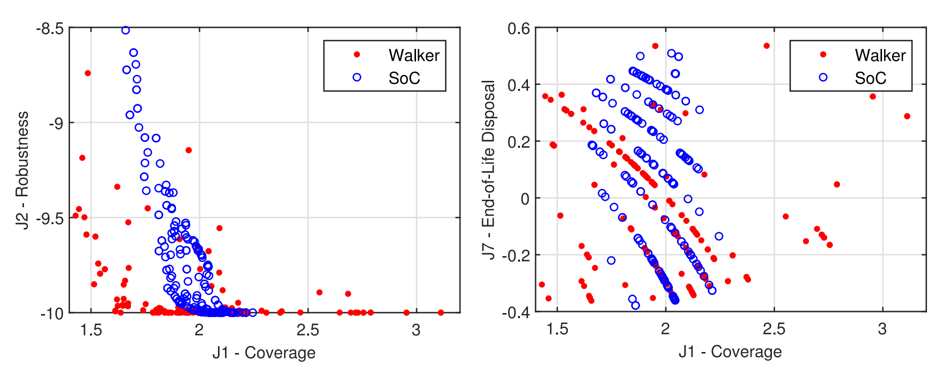

(a) J_1 versus J_2. **(b) J_1 versus $(J_7)_{\mathrm{MEO}}$.**

Fig. 18. Sensitivity analysis of objectives for the 4-fold MEO mission (dot: Walker, circle: SoC).

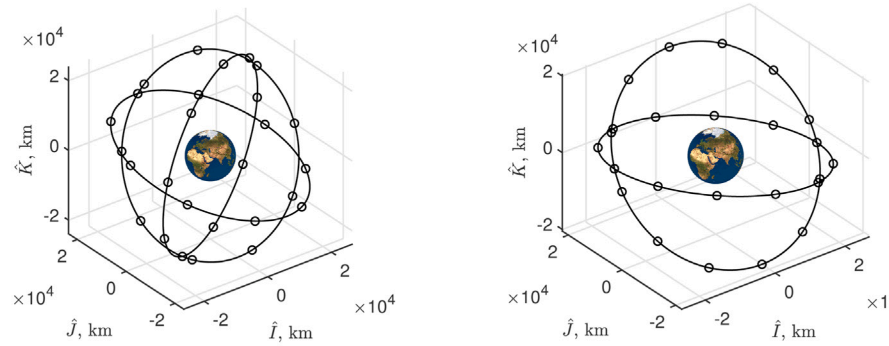

(a) Walker. (b) SoC.

Fig. 19. Alternatives to the GPS constellation.

Table 8
Results of the GPS and Galileo constellations and of the selected optimal constellations for the 4-fold MEO mission.

Symbol	GPS	Alternative GPS		Galileo	Alternative Galileo		New	
		Walker	SoC		Walker	SoC	Walker	SoC
N	24	27	24	24	27	24	18	24
P	6	3	2	3	3	2	3	2
F	2	1		1	1		2	
i, deg	55	64.6	49.8	56	62.4	78.5	61.3	76.4
h, km	20,200	20,065	20,379	23,222	23,122	23,588	27,903	26,177
J_1	1.80	2.02	1.80	1.86	2.09	1.87	1.46	1.92
J_2	−9.98	−10	−9.11	−10	−10	−9.48	−9.19	−9.59
J_3	1.27	1.15	1.01	1.06	1.10	0.98	1.11	0.96
J_4	1.09	1.23	0.99	1.13	1.23	1.36	1.17	1.36
J_5	6	3	2	3	3	2	3	2
$(J_7)_{\text{MEO}}$	−0.06	−0.01	−0.07	−0.13	−0.08	−0.14	−0.35	−0.20
cov	1.80	2.02	1.80	1.86	2.09	1.87	1.46	1.92
pct, %	99.83	100	91.08	100	100	94.79	91.86	95.88
opp, $\times10^{-3}$ s^{-1}	5.57	2.52	1.10	1.89	2.14	0.93	1.14	0.82
Ψ, deg	0	4.02	10.54	9.16	6.96	10.54	0.29	10.54
lch_h, $\times10^5$ km	4.85	5.42	4.89	5.57	6.24	5.66	5.02	6.28
lch_i, deg	49	58.65	43.79	50	56.38	72.48	55.27	70.43
bld	6	3	2	3	3	2	3	2
$(\Delta v_{\text{eol}})_{\text{MEO}}$, km/s	0.86	0.98	0.85	0.73	0.83	0.72	0.44	0.64

Among the optimal constellations, we select four constellations at similar altitudes of the GPS and Galileo constellations as the alternatives to GPS and Galileo, two for each, and another two new constellations at altitudes above 25,000 km so as not to interfere with the GPS and Galileo constellations. Apart from the altitude constraints, the following issues should also be considered during the selection.

(1) The selected constellations should have relatively fewer satellites, as the number of satellites is traditionally the prime cost driver for small- and middle-sized constellations [1, Table 13-2].
(2) The selected Walker constellations should have relatively fewer numbers of orbital planes, in order to speed up the build-up process to start the revenue flow as early as possible.

Table 8 presents the results of the GPS and Galileo constellations and of the selected optimal constellations. These results show that the selected constellations have advantages and disadvantages from different aspects, demonstrating again the need of trade-off for constellation design.

Figs. 19–21 show the configurations of the selected optimal constellations for the 4-fold MEO mission in the ECI coordinate system, where the round markers and lines indicate the satellites and orbital planes, respectively.

6. Conclusion

In this paper, a systematic method was developed for multi-criteria design of continuous global coverage Walker and SoC constellations, allowing seven critical constellation properties to be optimised in a traded off way, where the constellation properties refer to constellation performances or costs. In this method, the quantitative relationship between constellation configuration and properties was established. To be specific:

- the constellation configuration was represented by a set of characteristic parameters, with which all the configuration-related parameters of a Walker or SoC constellation can be determined;
- the constellation properties were quantitatively assessed by a series of indexes, where the indexes were modelled as functions of the characteristic parameters.

Moreover, this quantitative relationship also revealed the influence of constellation configuration on properties and thus helped analyse the trade-offs between properties. Based on the quantitative relationship, a multi-objective optimisation problem was formulated and then solved with the support of a multi-objective global optimiser. By replacing the mission-related parameters of the multi-objective optimisation problem with required values, the proposed method can be promptly applied to the multi-criteria design for any mission. As an implementation of the proposed method, some globally optimal constellations were found for a 1-fold LEO mission and for a 4-fold MEO mission; compared to the existing constellations (Iridium, GPS, and Galileo), the new designed constellations showed advantages and disadvantages from different aspects, demonstrating the need of trade-off for constellation design.

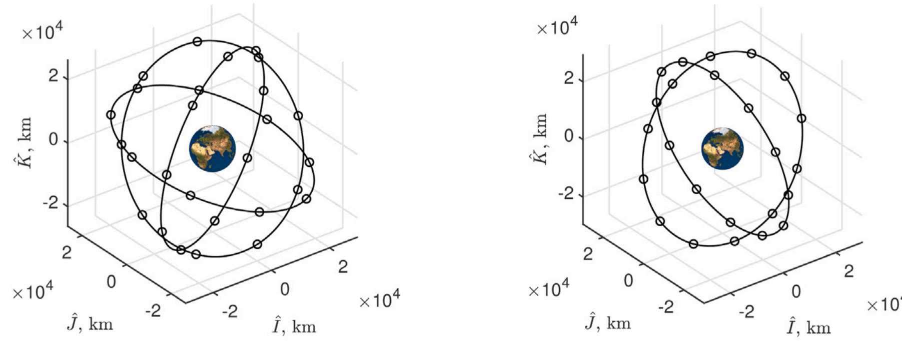

(a) Walker. **(b) SoC.**

Fig. 20. Alternatives to the Galileo constellation.

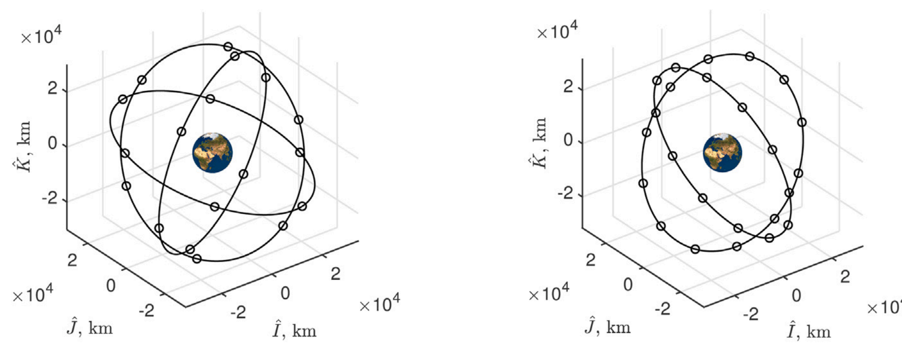

(a) Walker. **(b) SoC.**

Fig. 21. New constellations for the 4-fold MEO mission.

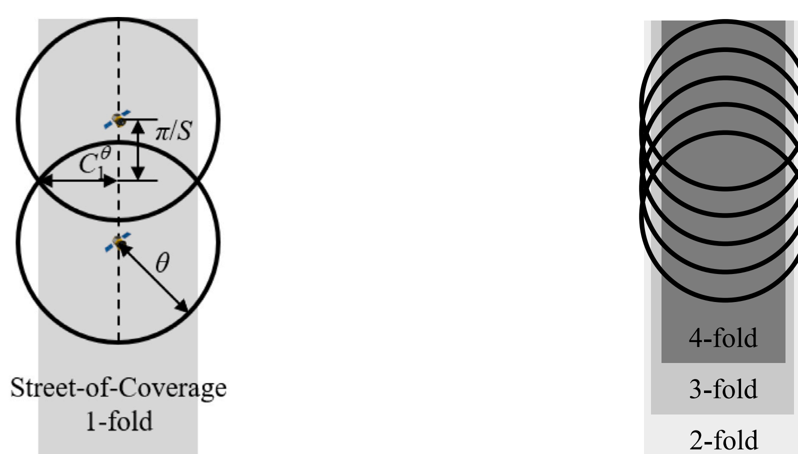

(a) Single-fold continuous coverage. **(b) Multiple-fold continuous coverage.**

Fig. 22. Coverage geometry of SoC.

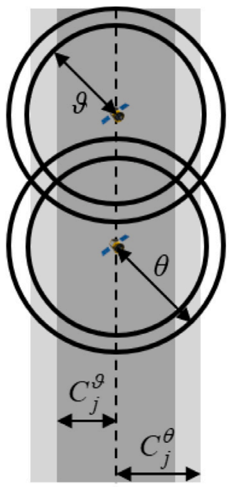

Fig. 23. Difference between the real and minimum half-widths of SoC.

Funding sources

The work performed for this paper has received funding from the European Research Council (ERC) under the European Union's Horizon 2020 research and innovation program (grant agreement No 679086 – COMPASS).

Declaration of competing interest

The authors declare that they have no known competing financial interests or personal relationships that could have appeared to influence the work reported in this paper.

Acknowledgments

The authors thank Mr. Thomas J. Lang for his kind help sharing his work "Optimal Low Earth Orbit Constellations for Continuous Global Coverage", which was used to determine the central angle of coverage for the Walker constellation. S. Huang acknowledges the National Natural Science Foundation of China (Grant agreement No 61903214) and the Chinese Government Scholarship awarded by the Chinese Scholarship Council.

Appendix A. Coverage geometry of Street-of-Coverage concept

The SoC constellation was developed based on a Street-of-Coverage (SoC) concept. Fig. 22 illustrates the coverage geometry of SoC for a single orbital plane containing S evenly spaced satellites, where the circles with an angular radius of θ are the footprints projected onto the Earth's surface. As shown in Fig. 22(a), if $\theta \geq j\pi/S$, the coverage will be j-fold continuous along the swath with a half-width of C_j^{θ} (in Fig. 22(a), $j = 1$), and such swath is called the Street-of-Coverage, indicated by the shadow area. θ and C_j^{θ} are related by [8,18,19]

$$\cos\theta = \cos C_j^{\theta} \cos(j\pi/S) \tag{35}$$

Fig. 22(b) shows that the higher the coverage fold, the narrower the SoC will be.

It is of note that C_j^{θ} is the real half-width of SoC, however, the determination of $\Delta\Omega_{\text{co}}$ and $\Delta\Omega_{\text{counter}}$, along with Δu_{inter}, depends on the minimum half-width of SoC required for j-fold continuous coverage, that is, C_j^{ϑ} given in Eq. (3). Fig. 23 shows the difference between the real and minimum half-widths of SoC.

Appendix B. Coverage geometry of co- and counter-interfaces

Fig. 24 illustrates the coverage geometry of the co- and counter-rotating interfaces for j-fold continuous coverage, where the arrows along the dashed lines indicate the direction of satellite motion and the shadow areas indicate the co- and counter-rotating interfaces. For the co-rotating interface, as shown in Fig. 24(a), the relative positions of satellites do not change over time, and thus the coverage dips can always be offset by the coverage bulges if the perpendicular angular separation between orbital planes are set to $(\vartheta + C_j^{\vartheta})$. For the counter-rotating interface, as shown in Fig. 24(b), the relative positions of satellites change over time, and thus to ensure the coverage being continuous along the interface, the perpendicular angular separation between orbital planes has to be narrowed to $(C_1^{\vartheta} + C_j^{\vartheta})$, although leading to large coverage overlaps.

Note that here the perpendicular angular separation is not the RAAN spacing but is an arc on the great circle 90 deg from the intersection of two orbits [1, Sec. 13.1]; the RAAN spacing $\Delta\Omega$ and the perpendicular angular separation D are related by [1, Sec. 13.1]

$$\sin\frac{\Delta\Omega}{2} = \sin\frac{D}{2} / \sin i \tag{36}$$

Appendix C. Approaches to determining central angle of coverage

In the following we will introduce the approaches to determining the central angle of coverage ϑ for Walker and SoC constellations.

C.1. Walker constellations

For the Walker constellation, there are two typical approaches to determining ϑ: the "circumcircle" approach [4–6,11] and the "test point" approach [13].

In the "circumcircle" approach, the Earth's surface is divided into a series of non-overlapping triangles, each triangle formed by three sub-satellite points, and the combination of non-overlapping triangles changes over time. At each time interval, the angular radii of the circumcircles of non-overlapping triangles can be computed. Then the size of the central angle of coverage can be determined by the largest circumcircle over all time intervals in one orbit period. However, the work of finding non-overlapping triangles for every time interval is computationally expensive, and thus the "circumcircle" approach does not suit constellations containing large numbers of satellites.

Compared to the "circumcircle" approach, the "test point" approach is more computationally efficient. In the "test point" approach, a virtual Earth,[6] which rotates at the same rate as the constellation, is introduced, and any Walker constellation can be regarded as "geosynchronous" with respect to the virtual Earth. Due to the symmetry of the Walker constellation, the surface of the virtual Earth can be divided into several regions by the groundtracks of the "geosynchronous" constellation, all regions having the same coverage pattern. Thus, only one of the regions needs to be considered. Then generating a set of test points in any of the regions and within that region, computing the angular distances between the test points and sub-satellite points for all time intervals in one orbit period, the central angle of coverage can be determined by the minimum angular distance that ensures all test points visible at any instant.

[6] If the global Earth can be continuously covered by a constellation, then it will be continuously covered independent of the Earth's rotational rate [13].

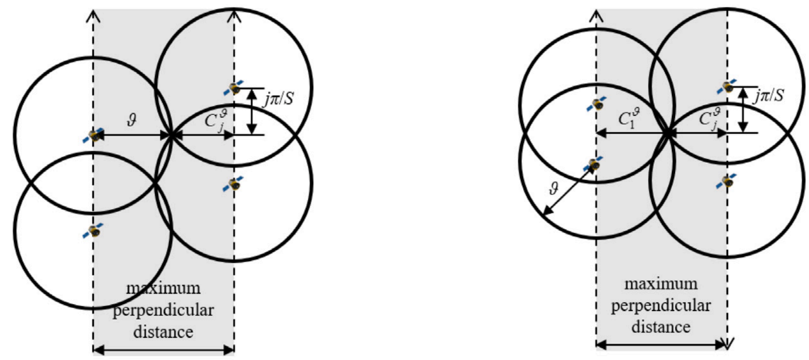

(a) Co-rotating interface.   **(b) Counter-rotating interface.**

Fig. 24. Coverage geometry of the co- and counter-rotating interfaces.

C.2. Street-of-Coverage constellations

For the SoC constellation, ϑ can be determined by solving the following equation

$$(P-1)\sin^{-1}\left(\sin\frac{\vartheta+C_j^{\vartheta}}{2}/\sin i\right)=\sin^{-1}\left(\sin\frac{\pi-C_1^{\vartheta}-C_j^{\vartheta}}{2}/\sin i\right) \tag{37}$$

which is derived by substituting Eq. (2) into Eq. (4). C_j^{ϑ} is a function of ϑ, j, and S (see Eq. (3)). If the characteristic parameters N, P, and i, as well as the required coverage fold j are given, Eq. (37)'s only unknown parameter will be ϑ, and it can be rapidly solved with the support of numerical optimisers such as the MATLAB nonlinear solver *fsolve* [42]. Note that Eq. (37) will not have solution if Eq. (11), the necessary condition for the SoC constellation able to offer a specified fold of continuous global coverage, is not satisfied.

References

[1] J.R. Wertz (Ed.), Mission geometry; orbit and constellation design and management, Microcosm Press and Kluwer Academic Publishers, 2001.
[2] X. Pan, M. Xu, R. Santos, Trajectory optimization for solar sail in cislunar navigation constellation with minimal lightness number, Aerosp. Sci. Technol. 70 (2017) 559–567, http://dx.doi.org/10.1016/j.ast.2017.08.042.
[3] X. Pan, M. Xu, Cislunar navigation constellation by displaced solar sails, J. Navig. 70 (2017) 963–982, http://dx.doi.org/10.1017/S037346331700025X.
[4] J.G. Walker, Circular Orbit Patterns Providing Continuous Whole Earth Coverage, Royal Aircraft Establishment, 1970.
[5] J.G. Walker, Some circular orbit patterns providing continuous whole earth coverage, J. Br. Interplanet. Soc. 24 (1971) 369–384.
[6] J.G. Walker, Continuous Whole-Earth Coverage by Circular-Orbit Satellite Patterns, Royal Aircraft Establishment, 1977.
[7] J.G. Walker, Coverage Predictions and Selection Criteria for Satellite Constellations, Royal Aircraft Establishment, 1982.
[8] Y. Ulybyshev, Near-polar satellite constellations for continuous global coverage, J. Spacecr. Rockets 36 (1) (1999) 92–99, http://dx.doi.org/10.2514/2.3419.
[9] G.V. Mozhaev, The problem of the continuous earth coverage and the kinematically regular satellite networks, I, Kosm. Issled. 10 (6) (1972) 833–840.
[10] G.V. Mozhaev, The problem of the continuous earth coverage and the kinematically regular satellite networks, II, Kosm. Issled. 11 (1) (1973) 59–69.
[11] A.H. Ballard, Rosette constellations of earth satellites, IEEE Trans. Aerosp. Electron. Syst. AES-16 (5) (1980) 656–673, http://dx.doi.org/10.1109/TAES.1980.308932.
[12] T.J. Lang, Symmetric circular orbit satellite constellations for continuous global coverage, in: AAS/AIAA Astrodynamics Specialist Conference, Kalispell, MT, U.S.A., 1987.
[13] T.J. Lang, Optimal low earth orbit constellations for continuous global coverage, in: AAS/AIAA Astrodynamics Specialist Conference, Victoria, BC, Canada, 1993.
[14] T.J. Lang, W.S. Adams, A comparison of satellite constellations for continuous global coverage, in: Mission Design & Implementation of Satellite Constellations, Dordrecht, 1998, pp. 51–62.
[15] R.D. Lüders, Satellite networks for continuous zonal coverage, Amer. Rocket Soc. J. 31 (2) (1961) 179–184, http://dx.doi.org/10.2514/8.5422.
[16] R.D. Lüders, L.J. Ginsberg, Continuous zonal coverage – A generalized analysis, in: Mechanics and Control of Flight Conference, Anaheim, CA, U.S.A, 1974, http://dx.doi.org/10.2514/6.1974-842.
[17] L. Rider, Analytic design of satellite constellations for zonal earth coverage using inclined circular orbits, J. Astronaut. Sci. 35 (1986) 31–64.
[18] D.C. Beste, Design of satellite constellations for optimal continuous coverage, IEEE Trans. Aerosp. Electron. Syst. AES-14 (3) (1978) 466–473, http://dx.doi.org/10.1109/TAES.1978.308608.
[19] L. Rider, Optimized polar orbit constellations for redundant earth coverage, J. Astronaut. Sci. 33 (1985) 147–161.
[20] D. Mortari, M.P. Wilkins, C. Bruccoleri, The flower constellations, J. Astronaut. Sci. 52 (1) (2004) 107–127.
[21] M.E. Avendaño, J.J. Davis, D. Mortari, The 2-D lattice theory of flower constellations, Celestial Mech. Dynam. Astronom. 116 (2013) 325–337, http://dx.doi.org/10.1007/s10569-013-9493-8.
[22] J.J. Davis, M.E. Avendaño, D. Mortari, The 3-D lattice theory of flower constellations, Celestial Mech. Dynam. Astronom. 116 (2013) 339–356, http://dx.doi.org/10.1007/s10569-013-9494-7.
[23] J.E. Draim, T.J. Kacena, Populating the abyss - investigating more efficient orbits, in: Proceedings of the Small Satellite Conference, 1992, https://digitalcommons.usu.edu/smallsat/1992/all1992/16/.
[24] E. Lansard, J. Palmade, Satellite constellation design: Searching for global cost-efficiency trade-offs, in: Mission Design & Implementation of Satellite Constellations, Dordrecht, 1998, pp. 23–31.
[25] E. Lansard, E. Frayssinhes, J. Palmade, Global design of satellite constellations: A multi-criteria performance comparison of classical walker patterns and new design patterns, Acta Astronaut. 42 (9) (1998) 555–564, http://dx.doi.org/10.1016/S0094-5765(98)00043-5.
[26] H. Keller, H. Salzwedel, G. Schorcht, V. Zerbe, Geometric aspects of polar and near polar circular orbits for the use of intersatellite links for global communication, in: 48th IEEE Vehicular Technology Conference. Pathway To Global Wireless Revolution (Cat. No. 98CH36151), vol. 1, Ottawa, ON, Canada, 1998, pp. 199–203.
[27] M.P. Ferringer, D.B. Spencer, Satellite constellation design tradeoffs using multiple-objective evolutionary computation, J. Spacecr. Rockets 43 (6) (2006) 1404–1411, http://dx.doi.org/10.2514/1.18788.
[28] Y. Li, S. Zhao, J. Wu, A general evaluation criterion for the coverage performance of leo constellations, Aerosp. Sci. Technol. 48 (2012) 94–101, http://dx.doi.org/10.1016/j.ast.2015.11.003.
[29] T. Shtark, P. Gurfil, Regional positioning using a low earth orbit satellite constellation, Celestial Mech. Dynam. Astronom. 130 (2) (2018) 1–28, http://dx.doi.org/10.1007/s10569-017-9811-7.
[30] P.G. Buzzi, D. Selva, N. Hitomi, W.J. Blackwell, Assessment of constellation designs for earth observation: Application to the TROPICS mission, Acta Astronaut. 161 (2019) 166–182, http://dx.doi.org/10.1016/j.actaastro.2019.05.007.
[31] https://www.esa.int/Applications/Navigation/Galileo/What_is_Galileo Retrieved: 15 July 2020.
[32] Y.C. Hubbel, A comparison of the IRIDIUM and AMPS systems, IEEE Netw. 11 (2) (1997) 52–59, http://dx.doi.org/10.1109/65.580922.
[33] https://earth.esa.int/web/eoportal/satellite-missions/i/iridium-next Retrieved: 10 December 2020.
[34] https://www.nasa.gov/directorates/heo/scan/communications/policy/GPS.html Retrieved: 15 July 2020.
[35] L.E. Speckman, T.J. Lang, W.H. Boyce, An analysis of the line of sight vector between two satellites in common altitude circular orbits, in: AIAA/AAS Astrodynamics Conference, Portland, OR, U.S.A., 1990, http://dx.doi.org/10.2514/6.1990-2988.
[36] J.R. Wertz, W.J. Larson (Eds.), Space mission analysis and design, third ed., Microcosm Press and Kluwer Academic Publishers, 1999.
[37] https://en.wikipedia.org/wiki/PSLV-C37 Retrieved: 10 December 2020.
[38] D.A. Vallado (Ed.), Fundamentals of astrodynamics and applications, second ed., Microcosm Press and Kluwer Academic Publishers, 2004.

[39] C. Lücking, C. Colombo, C.R. McInnes, A passive satellite deorbiting strategy for medium earth orbit using solar radiation pressure and the J2 effect, Acta Astronaut. 77 (2012) 197–206, http://dx.doi.org/10.1016/j.actaastro.2012.03.026.

[40] C. Lücking, C. Colombo, C.R. McInnes, Solar radiation pressure-augmented deorbiting: Passive end-of-life disposal from high-altitude orbits, J. Spacecr. Rockets 50 (6) (2013) 1256–1267, http://dx.doi.org/10.2514/1.A32478.

[41] M. Vasile, Robust mission design through evidence theory and multi-agent collaborative search, Ann. New York Acad. Sci. 1065 (1) (2005) 152–173, http://dx.doi.org/10.1196/annals.1370.024.

[42] https://uk.mathworks.com/help/optim/ug/fsolve.html Retrieved: 15 November 2020.